2006

INTERACTIONS BETWEEN VASP AND METAVINCULIN

Sarah D. Aubut
Western University

INTERACTIONS

BETWEEN

VASP AND METAVINCULIN

(Thesis format: Monograph)

by

Sarah D. Aubut

Graduate Program
In the
Department of Biochemistry

A thesis submitted in partial fulfillment
of the requirements for the degree of
Master of Science

Faculty of Graduate Studies
The University of Western Ontario
London, Ontario, Canada

THE UNIVERSITY OF WESTERN ONTARIO
FACULTY OF GRADUATE STUDIES

CERTIFICATE OF EXAMINATION

Supervisor	Examiners
Dr. Eric H. Ball	Dr. Brian Shilton
Supervisory Committee	Dr. James Choy
Dr. David Edgell	Dr. Lina Dagnino
Dr. David Litchfield	

The thesis by

Sarah Dawn Aubut

entitled:

Interactions Between VASP and Vinculin

is accepted in partial fulfillment of the
requirements for the degree of
Master of Science

Date_____

_____
Chair of the Thesis Examination Board

ABSTRACT

Vinculin and metavinculin are components of cell-matrix and cell-cell adherens junctions, differing in a 68 residue insert in the metavinculin C-terminus. These proteins are known to interact with the EVH1 domain of VASP through a proline-rich motif. A second probable proline-rich motif was identified in the metavinculin insert.

The intent of this study was to determine whether a second motif in the metavinculin insert was a VASP binding site. A number of solution phase assays proved unable to detect an interaction through either site, but a solid-phase, overlay assay could do so. Mutations in the two motifs were constructed and VASP binding measured. Both motifs were found to contribute to the binding. A fluorescent probe was able to restore binding to both motifs in place of the native phenylalanine. Thus, it appears that the insert proline-rich motif may be a VASP binding site.

Keywords: vinculin C-terminus, metavinculin C-terminus, VASP, overlay assay, EVH1

to my family and friends

ACKNOWLEDGMENTS

I would like to thank Dr. Eric Ball for his unwavering support, patience, and guidance. Your expertise was matched only by your optimism, and you have been an inspiration by sharing your steadfast love for science with all.

I would like to thank my committee members, Dr David Litchfield and Dr. David Edgell for all the insightful suggestions throughout the project.

I would like to thank Barb Green, Melita Hayes and Debbie Coban for all their assistance over the past two years.

I would like to thank all the past and present Ball lab members for helping me whenever I was in a jam, and for tolerating my endless singing.

I would like to thank my family, friends and Chloe for keeping me sane and for the unfaltering faith in me; I could not have done this without you!

TABLE OF CONTENTS

LIST OF TABLES

LIST OF FIGURES

LIST OF ABBREVIATIONS

Arp	actin – related protein
BCIP	5 – bromo – 4 – chloro – 3 – indolyl phosphate
Cf	cysteine free
CPM	7 – diethylamino – 3 – (4' – maleimidyl – phenyl) – 4 – methylcoumarin
Da	dalton
DTNB	5, 5' – dithio – bis (2 – nitrobenzoic acid)
DTT	dithiothreitol
EDTA	ethylene glycol – bis (β – aminoethyl ether)
Ena	*Drosophila* enabled
EVH1	Ena/VASP homology 1
EVH2	Ena/VASP homology 2
Evl	Ena/VASP like
FPLC	fast protein liquid chromatography
GST	glutathione – S – tranferase
IP_6	inositol hexaphosphate
IPTG	isopropyl – β – D – thiogalactoside
kDa	kilodalton
KG	pGEX-KG vector
KG-T	modified KG vector with a TEV cleavage site
Mena	murine enabled
mVt	metavinculin C-terminal tail (833 – 1134)
NBT	nitro blue tetrazolium
NPM	N-(1-pyrenyl) maleimide
PBS	phosphate buffered saline
PCR	polymerase chain reaction
PH	pleckstrin homology
PI	phosphatidylinositol
PIP_2	phosphatidylinositol 4,5 – bisphosphate
p.s.i.	pounds per square inch

site 1	residues 842 – 846
site 2	residues 939 – 943 (metavinculin only)
SDS	sodium dodecylsulphate
SDS-PAGE	sodium dodecylsulphate polyacrylamide gel electrophoresis
TBS	tris buffered saline
TEV	tobacco etch virus
Tris	tris-(hydoxymethyl) aminomethane
Trx	thioredoxin
UWO	University of Western Ontario
VASP	vasodilator-stimulated phosphoprotein
Vh	vinculin head (1 – 835)
Vt833	vinculin C-terminal tail (833 – 1066)
Vt877	vinculin C-terminal tail (877 – 1066)
Wt	wild type

CHAPTER 1

INTRODUCTION

1.1. Overview

Cellular adhesion can occur between neighbouring cells, as well as between a cell and the extracellular matrix (ECM), and these connections are essential for many different cellular processes, including migration, differentiation and spreading (Zamir and Geiger 2001). Cellular adhesion is mediated by complexes of proteins, which are composed of transmembrane proteins, plus cytoskeletal proteins, both of which are essential in linking the actin cytoskeleton to other cells or to the ECM.

Of the numerous proteins found in these adhesion complexes, one of them is vinculin, from the Latin word *vinculum*, to link (Geiger, et al. 1980). Vinculin has been shown to bind to certain cytoskeletal and signalling proteins, as well as to acidic phospholipids. Metavinculin, a splice variant of vinculin, is also known to interact with many of the same ligands, despite an extra 68 amino acid insert in its C-terminus (Strasser, et al. 1993). Another key difference between these two isoforms is in their expression, with vinculin being ubiquitously expressed, while metavinculin is primarily found in smooth and cardiac muscle (Belkin, et al. 1988). Interestingly, there have been mutations identified in metavinculin that are correlated with cardiomyopathies (Maeda, et al. 1997; Olson, et al. 2002).

One of the many ligands for the vinculin proteins is VASP (vasodilator stimulated phosphoprotein), which is another of the many proteins found at adhesion sites, and is involved in the regulation of actin polymerization (Krause, et al. 2003). The N-terminal domain of VASP is involved in the interaction with the vinculin proteins, which involves

a proline-rich site in vinculin (Reinhard, et al. 1996). VASP has also been implicated in cardiomyopathies (Eigenthaler, et al. 2003).

1.2. Vinculin

1.2.1. Structure

Vinculin, a 117 kDa cytoskeletal protein, is ubiquitously expressed, is highly conserved and is a component of both cell-cell and cell-ECM junctions. There are three distinct domains in this protein: a large, globular N-terminal head (residues 1-835), a central, proline-rich hinge (residues 836-876) and a C-terminal tail (residues 877-1066). The complete crystal structure of the chicken protein was recently solved (Bakolitsa, et al. 2004; Borgon, et al. 2004), (Figure 1.1). This structure shows an N-terminal head domain (Vh) composed of seven, four-helix bundles that encircle a five-helix bundle C-terminal tail (Vt). A portion of the proline-rich hinge (856-874) was not resolved in the crystal, most likely due to its flexibility. This structure shows vinculin in a closed conformation, where there are strong contacts occurring between the head and tail. Vinculin is known to exist in at least two different conformations, which are important in mediating ligand interactions – a closed, or inactive form, and an open, active form in which the head and tail domains are dissociated (Bakolitsa, et al. 2004; Johnson and Craig 1994).

1.2.2. Function

Vinculin has no enzymatic activity, but it does contain many binding sites for a number of ligands, which include talin (Cohen, et al. 2006), α-actinin (Kelly, et al. 2006) and α-catenin (Yamada, et al. 2005), all of which interact with the Vh. The proline-rich hinge has binding sites for VASP (Brindle, et al. 1996), the Arp 2/3 complex (DeMali,

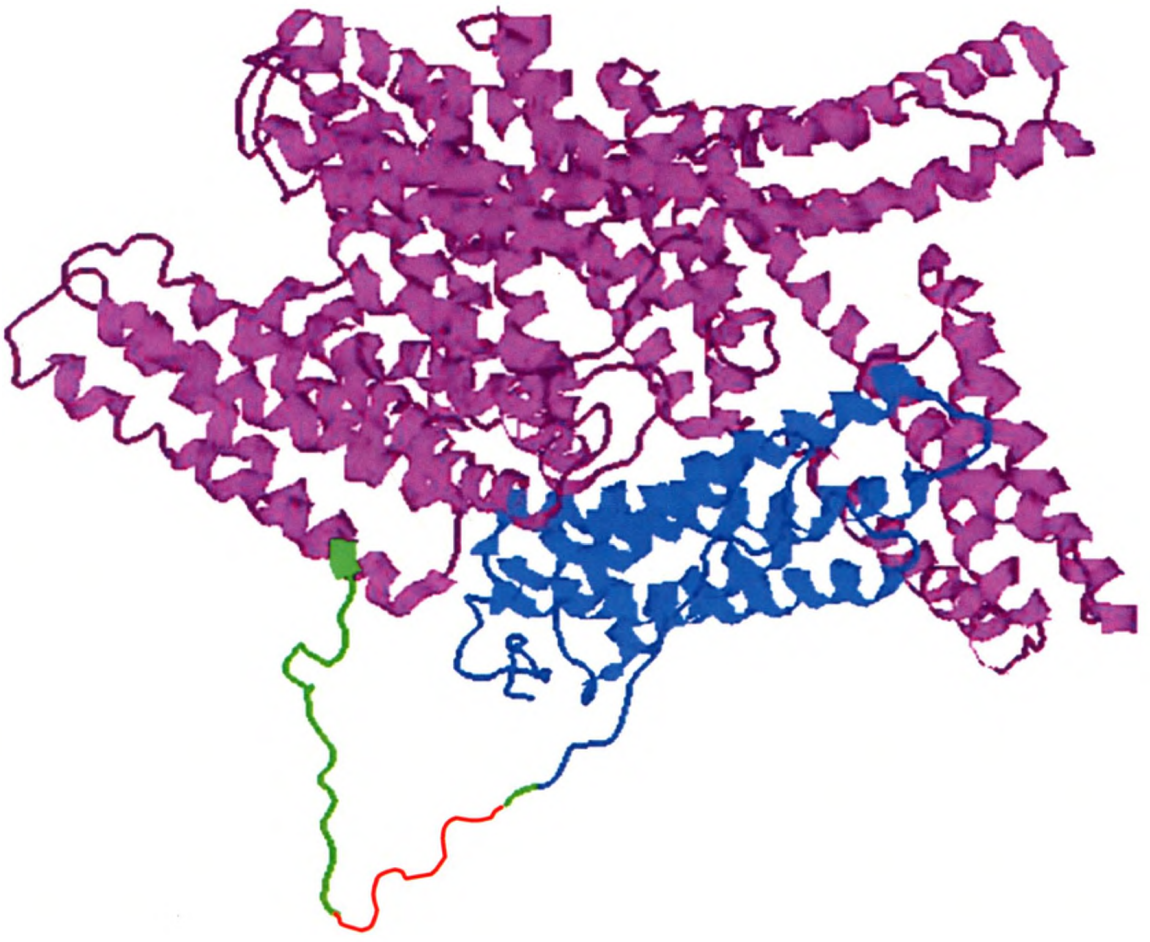

Figure 1.1: Cartoon diagram from the crystal structure of full-length chicken vinculin (PDB ID: 1ST6, (Bakolitsa, et al. 2004)). The domains are coloured as follows: N-terminal head (1-835) – purple, proline rich hinge (836-876) – green, C-terminal tail (877-1066) – blue. A segment of the proline rich hinge (856-874) was not resolved in the crystal; this was drawn in using Microsoft Word and is shown in red.

Barlow and Burridge 2002), ponsin (Mandai, et al. 1999) and vinexin (Kioka, et al. 1999). Vt is known to interact with F-actin (Janssen, et al. 2006), paxillin (Wood, et al. 1994) and acidic phospholipids (Johnson, et al. 1998; Weekes, Barry and Critchley 1996). For vinculin to bind some of these ligands, the protein must first be in its open, active conformation. Binding of ligands triggers a conformational switch in vinculin, although the mechanism by which the switch occurs is unknown. A number of the binding partners have been proposed to be involved, such as talin, α-actinin, and PIP_2 (Bois, et al. 2006; Weekes, Barry and Critchley 1996).

Vinculin was first identified as a contaminant in an α-actinin purification from chicken gizzard, and was found to be localized to the termini of stress fibres in cultured cells (Geiger 1979). Since this initial discovery, a great deal about how vinculin functions has been revealed. The role of vinculin in living cells has been investigated through the use of vinculin knockouts, in both cell and mouse models. In the embryonic stem cell knockouts, there was a change in the cell morphology, with a rounder shape compared to the wild-type, and there was also a marked decrease in adhesion and spreading, accompanied by a more than 2-fold increase in cell motility (Coll, et al. 1995). These vinculin-null cells were still able to differentiate into a variety of different cell types found in early embryogenesis, implying vinculin is not required at this stage. However, in the mouse model, a complete loss of vinculin resulted in lethality at day 10, with embryos being 30-40% smaller than wild-type, having retarded limbs, as well as sparse and fragile ectodermal tissues (Xu, Baribault and Adamson 1998). As there were notable neural and cardiac defects in the knockouts, vinculin may also play an important role in the development of these specific systems. In C. elegans, a loss of vinculin resulted in complete muscle paralysis, as well as lethaility at larval L1 stage (Barstead and Waterston

1991), implying that vinculin is essential for muscle function in nematodes, as well as further emphasizing the importance of vinculin in developmental processes.

One notable aspect of the vinculin knockout cells is that they are still able to assemble focal adhesions comparable to that of wild-type cells (Volberg, et al. 1995). Despite these apparently normal focal adhesions, they spread more slowly, and to a lesser extent, and they also close a wound much more rapidly than the wild-type cells (Saunders, et al. 2006). The focal adhesions were in fact smaller than those from vinculin-containing cells and less abundant, with a higher turn-over rate. Overexpression of vinculin results in the opposite change in cell motility, with a decrease in locomotion and an impairment of the ability to close a wound (Rodriguez Fernandez, et al. 1992). Thus, vinculin does not seem to be essential for focal adhesion formation but does negatively regulate cell migration.

How exactly vinculin is regulating these processes is still unknown, but it is believed that it depends on interaction with some of its ligands. Recent research has shed some light on the role vinculin plays in focal adhesion turnover, where it was found that it functions as a sensor of PIP_2 levels, which is thought to regulate the uncoupling of adhesion sites (Chandrasekar, et al. 2005). A great deal of what is occurring with vinculin in cells still needs to be discovered, but the information to date highlights the importance of vinculin in cell spreading, the proper assembly of large focal adhesions and in the suppression of cell migration.

1.3. Metavinculin

1.3.1. Sequence and role

Metavinculin is a splice variant of vinculin, the difference between them being an extra 68 amino acid insert, found between helices one and two of the Vt domain (Figure 1.2A and B) (Weller, et al. 1990). The insert region can be divided into two regions: an N-terminal variable region, and a C-terminal, highly conserved region (Figure 1.2B) (Strasser, et al. 1993).

The functional difference between vinculin and metavinculin is still unknown, as no metavinculin-specific ligands have been identified. However, it has been shown that the tail domains of the two variants have different F-actin bundling properties (Olson, et al. 2002), which implies some difference in the conformation of the metavinculin tail, as the F-actin binding site is not in the insert. The tail domains of the two isoforms also have different affinities for the head domain, with metavinculin having an association constant approximately nine times lower than that of vinculin (Witt, et al. 2004). Acidic phospholipids are involved in exposing cryptic oligomerization sites in the tail domain of vinculin, but this is not believed to occur in metavinculin, which was shown to have reduced binding to phospholipids, and in turn, reduced oligomerization compared to vinculin (Izard, et al. 2004; Witt, et al. 2004). This decrease in lipid binding was restored when acidic residues in the insert were mutated to uncharged residues. Metavinculin was, however, readily incorporated into heterodimers with phospholipid-activated vinculin (Witt, et al. 2004), implying vinculin may be involved in activating its isoform. It is notable that metavinculin is found mainly in smooth and cardiac muscle where it is co-expressed with vinculin (Belkin, et al. 1988). A novel ligand protein, raver1, was shown to have a higher affinity for metavinculin over vinculin, despite the fact it is not directly

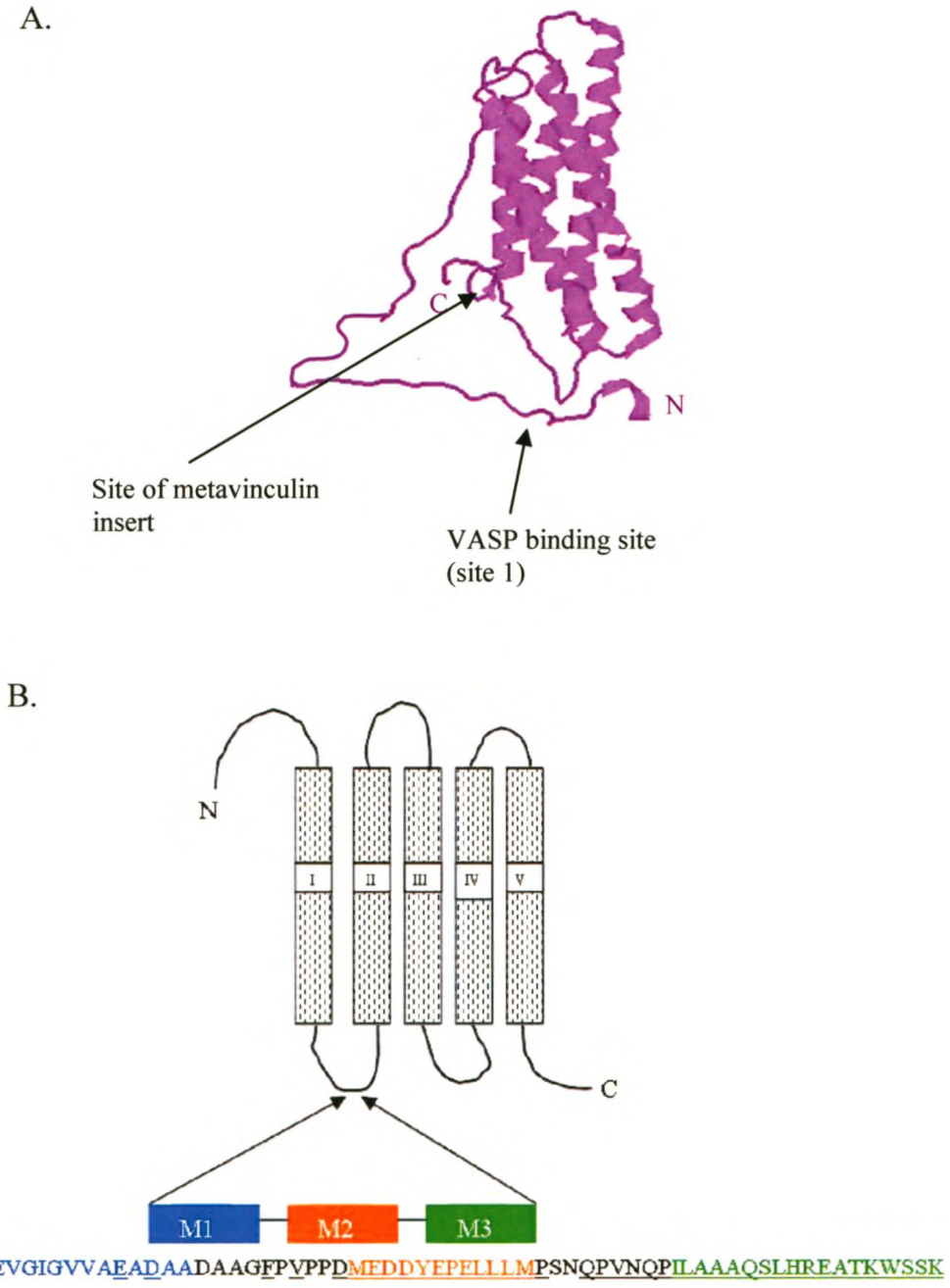

Figure 1.2: Site and sequence of metavinculin insert. A. Cartoon of crystal structure of vinculin tail (833-1066), indicating insert site and VASP binding site. B. Cartoon diagram of vinculin tail, showing the proposed structure of metavinculin insert (Olson, et al. 2002). M1, M2 and M3 are probable metavinculin helices. Insert sequence is shown, with residues coloured to match proposed structure, and conserved residues underlined.

interacting with the insert (Huttelmaier, et al. 2001). It seems logical that metavinculin should have some function distinct from vinculin that has yet to be discovered.

1.3.2. DCM causing mutations

Dilated cardiomyopathy (DCM) is a disease of the heart that is characterized by dilation and impaired contraction of the left ventricle or both ventricles (Richardson, et al. 1996). The majority of DCM cases involve a mutation in the proteins present in the cardiac myocyte, which include those associated with the sarcomere, cytoskeleton and the sarcolemma (Chang and Potter 2005). A large number of proteins can be mutated to give the same DCM phenotype. Among the proteins that have been identified as having mutations are dystrophin, β-myosin heavy chain, δ-sarcoglycan, cardiac actin, and metavinculin (Fatkin and Graham 2002). In a screening of patients with idiopathic DCM, two specific mutations in the metavinculin insert were identified: R975W and L954del (Olson, et al. 2002). A third mutation, in which the metavinculin isoform is completely absent, leaving only vinculin, was also identified in a patient with idiopathic DCM (Maeda, et al. 1997). Recently, the R975W mutation was identified in a patient with hypertrophic cardiomyopathy (HCM), which is characterized by hypertrophy of the left ventricle or both ventricles (Vasile, et al. 2006). It is believed that HCM and DCM are partially allelic disorders, as other mutations first identified in DCM have also been found in patients with HCM. The occurrence of metavinculin-specific mutants in DCM and HCM patients suggests that metavinculin has a specific function(s) distinct from that of vinculin, but the nature of this function(s) is unknown.

1.4. VASP

Vasodilator-stimulated phosphoprotein (mammalian VASP) is one of the founding members of the Ena/VASP family of proteins, which includes *Drosophila* Ena (enabled), *C.elegans* Unc-34, *Dictyostelium* DdVASP, mEna (murine enabled), and Evl (mammalian Ena/VASP-like) (Krause, et al. 2003). This family of proteins share a conserved tripartite domain structure, comprised of an N-terminal Ena/VASP homology 1 (EVH1) domain, a central proline-rich region and a C-terminal Ena/VASP homology 2 (EVH2) domain. All members of this family have been identified as regulators of actin assembly and cell motility, and they are commonly found at the leading edge of migrating cells, as well as in focal adhesions, both sites of actin assembly (Bear, et al. 2000).

1.4.1. Structure

VASP is a 40kDa protein that was first identified by Halbrugge and Walter as a major phosphorylated protein in platelets and endothelial cells after stimulation with vasodilators, such as nitric oxide (NO) and prostaglandin I_2 (PGI_2), which raise levels of cGMP and cAMP respectively (Halbrugge and Walter 1989). Since then, VASP has been found to be expressed in a variety of cell types, including fibroblasts, macrophages, neuronal cells, smooth muscle cells, and endothelial cells, but is found at the highest concentrations in platelets (Krause, et al. 2003).

The different domains of VASP are functionally distinct (Figure 1.3). VASP has been shown to behave as a homotetramer in solution, an occurrence that is entirely dependent on the final 45 residues of the C-terminal EVH2 domain, which forms a right handed coiled coil (Kuhnel, et al. 2004; Zimmermann, et al. 2002). This domain is also involved in G-actin stabilization and nucleation, as well as in F-actin binding and

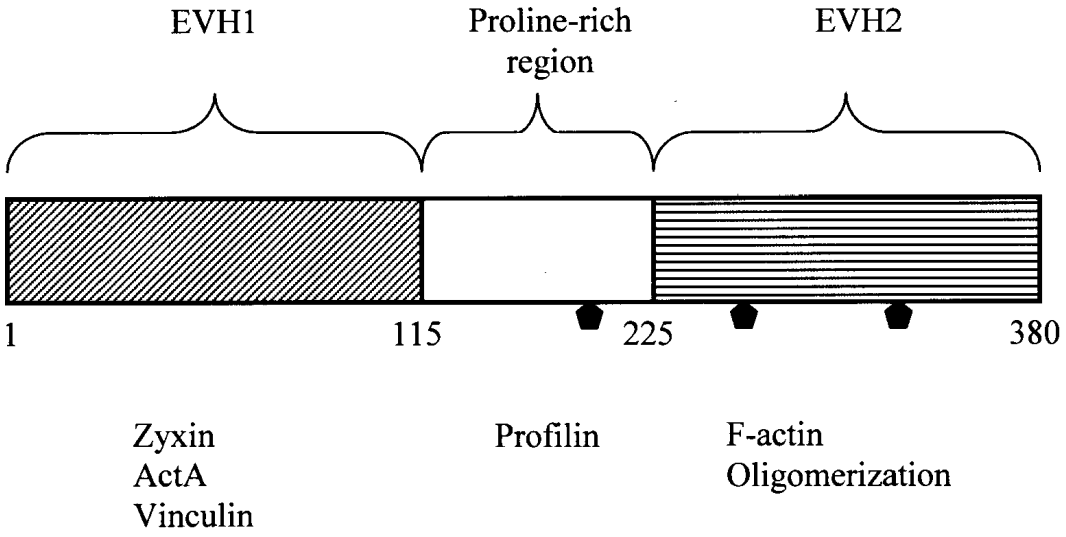

Figure 1.3. Linear diagram of VASP structure.
Interactors are shown beneath respective domain.
⬟-phosphorylation sites: S^{157}, S^{239} and T^{278}.

bundling (Bachmann, et al. 1999; Walders-Harbeck, et al. 2002). The central proline- rich domain harbours a proline rich binding site for both isoforms of profilin, which are small, G-actin binding proteins (Reinhard, et al. 1995), and this domain can also interact with SH3 and WW domain-containing proteins, such as Abl (Howe, Hogan and Juliano 2002), although the purpose of this interaction is not known.

The EVH1 domain is a 115-residue, N-terminal domain, and is a member of the pleckstrin homology (PH) domain superfamily, although, unlike the PH domain, it does not interact with phosphatidylinositol lipids (Ball, et al. 2002; Volkman, et al. 2002) (Figure 1.4). In contrast, the EVH1 domain interacts with proline-rich peptide ligands, with different families having different specificities. For example, the EVH1 domain in the Homer/Vesl family of postsynaptic receptor-associated proteins recognizes the core motif PPxxF, while the EVH1 domain from the Ena/VASP family recognize the core motif FPxφP, where x is any residue and φ is a hydrophobic residue (Ball, et al. 2002).

1.4.2. EVH1 domain-ligand interaction

The first protein identified as interacting with the EVH1 domain of VASP through a proline-rich site was ActA from *Listeria monocytogenes* (Chakraborty, et al. 1995). ActA is a surface protein on this bacterium that is essential for cell-to-cell spreading, and functions in actin recruitment that drives motility. ActA has four central Phe-Pro-Pro-Pro-Pro (FP_4) motifs, each of which has been shown to simultaneously interact *in vitro* with an EVH1 domain (Machner, et al. 2001; Niebuhr, et al. 1997). By binding to VASP, ActA is able to provide a continuous recruitment of actin that equips the bacterium with a comet-like tail that allows it to propel itself through the host cell (Domann, et al. 1992). Peptides of the four separate ActA FP_4 motifs have similar affinities for the EVH1

Figure 1.4: Cartoon diagram from the NMR spectroscopy of the EVH1 domain of human VASP (PDB ID: 1EGX, (Ball, et al. 2000)).

domain, all around 19μM (Ball, et al. 2000). Zyxin, another of the VASP ligands that interacts with the EVH1 domain, also contains four FP_4 motifs, but with a wider range of affinities between the sites, ranging from 74 to 197μM (Ball, et al. 2000; Niebuhr, et al. 1997). This lower affinity could be due to the fact that in three of the four motifs, the second or third residue is not a proline, but is instead a serine, lysine or alanine (Ball, et al. 2002). The FP_4 motif is key to the interaction with EVH1, but also of importance are residues flanking the core motif, including the residue immediately preceding the phenylalanine (1^{st}), and the fourth (4^{th}) and fifth (5^{th}) residue following the final proline (Figure 1.5). In ActA, which exhibits the highest affinity binding, the preceding residue and the fourth following residue are acidic, while the fifth residue is hydrophobic. These residues appear to play a role in strengthening the interaction with the EVH1 domain, as mutating the acidic residues to basic residues noticeably decreases the binding, while binding with peptides lacking all three of the residues reduced the binding to an undetectable level (Ball, et al. 2000; Carl, et al. 1999).

Other ligands for the EVH1 domain that have been identified include: migfilin, a widely expressed focal adhesion protein; PREL1 (proline rich EVH1 ligand), a protein found in lamellipodia; Fyb/SLAP, a protein involved in T cell activation; palladin, an actin-associated protein; lamellipodin, a protein found in lamellipodia; and LPP, a zyxin-related, actin-associated protein (Boukhelifa, et al. 2004; Jenzora, et al. 2005; Krause, et al. 2000; Krause, et al. 2004; Petit, et al. 2000; Zhang, et al. 2006). Another interaction of the EVH1 domain, the one that is the focus of this project, is with the vinculin proteins.

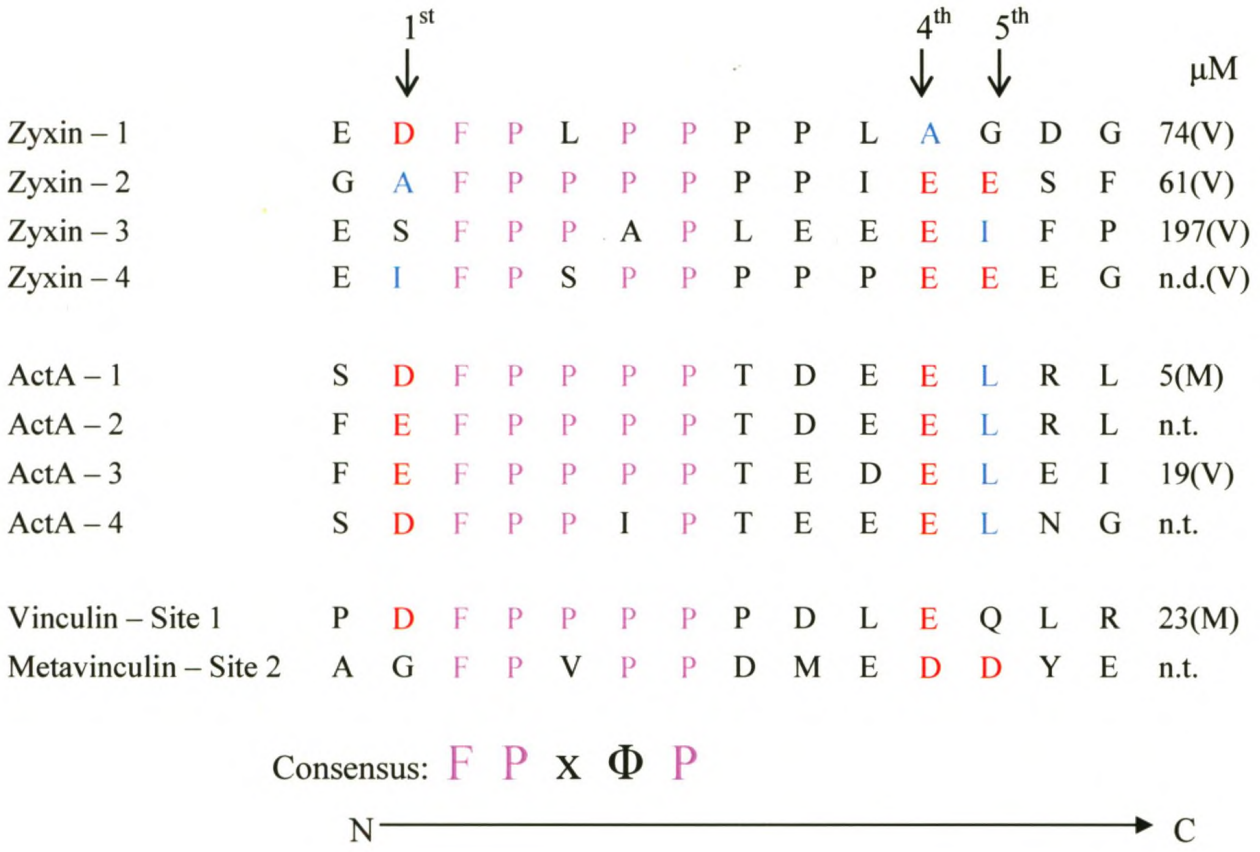

Figure 1.5: Sequences of EVH1 binding peptides found in zyxin, ActA and vinculin. The motif includes the central consensus sequence, as well as the flanking residues, with the significant residues indicated by an arrow. Binding constants were determined by fluorescence titration with VASP (V) (Ball, et al. 2000) or Mena (M) (Prehoda, Lee and Lim 1999). Acidic residues are shown in red, hydrophobic residues in blue, and consensus core in pink. n.d – no binding detected. n.t – binding not tested.

1.4.3. Function

As implied by the name, VASP has three known phosphorylation sites, one of which is Ser^{157} in the proline rich region. The other two sites (Ser^{239} and Thr^{278}) are located in the EVH2 domain (Butt, et al. 1994). An apparent shift in molecular weight of VASP from 46 to 50 kDa is correlated with phosphorylation at the preferred Ser^{157} (Halbrugge and Walter 1989). Phosphorylation of VASP has been shown to have a negative effect on both actin nucleation and filament binding and bundling, but with no apparent effect on tetramerization, or on interactions through the EVH1 domain (Harbeck, et al. 2000).

VASP proteins have been pinpointed as being important in actin filament formation, and are associated with actin at various locations such as focal adhesions, adherens junctions, lamellae, stress fibres, as well as in the intercalated disks in cardiomyocytes (Krause, et al. 2003). VASP is concentrated at the intercalated disks, along with its family member Mena, where it is believed to contribute to the functional and morphological integrity of cardiomyocytes (Towbin and Bowles 2006).

In an effort to understand the function of the VASP protein *in vivo*, knockouts have been employed. In mice, a loss of VASP resulted in hyperplasia of megakaryocytes in bone marrow and spleen, and cAMP and cGMP-mediated inhibition of platelet aggregation was significantly reduced, but no further abnormalities were seen (Aszodi, et al. 1999; Hauser, et al. 1999). Mena knockout in mice result in defects in the formation of a number of neural components, including the corpus callosum and both the dorsal and ventral hippocampal commissures (Lanier, et al. 1999). It is known that the different VASP family members can compensate for a lack in another of the family members (Aszodi, et al. 1999; Loureiro, et al. 2002), and so a double knockout of VASP and Mena

was attempted in mice. The mice died perinatally, exhibiting defects in neurulation, craniofacial structure, as well as in the formation of several tracts in both the central and peripheral nervous systems (Menzies, et al. 2004). Thus the VASP family of proteins are important for proper neural development.

The lethality of the double knockouts made studying the function of VASP and Mena in cardiac tissue a difficult task, but it was attempted through the use of a dominant negative strategy involving cardiac specific expression of the VASP EVH1 domain in mice. This overexpression of the EVH1 domain resulted in specific displacement of both VASP and Mena from the intercalated discs, and brought about dilated cardiomyopathy with myocyte hypertrophy and bradycardia. This ultimately led to early postnatal lethality to the mice with the highest expression of the EVH1 domain (Eigenthaler, et al. 2003). This result highlights the important role that VASP plays in regulating and maintaining actin processes in the highly specialized cells of the heart.

On the molecular level, VASP function has been suggested to involve the following mechanisms: anti-capping and anti-branching of actin filaments, as well as profilin recruitment. It has been shown that VASP increased the rate of actin polymerization in the presence of capping proteins, such as CapG and heterodimeric capping protein (CP) (Barzik, et al. 2005). This increased actin polymerization most likely involves the association of VASP with the filament at or near the barbed end, where the EVH2 domain on its own has been shown to be effective in preventing capping (Barzik, et al. 2005). Through the use of a mitochondria-targeted ActA peptide, levels of VASP and Mena were depleted at their normal locations in fibroblasts. This results in the formation of dense actin networks with highly-branched filaments. Contrastingly, increasing VASP leads to sparse networks with mostly long, unbranched filaments (Bear,

et al. 2002). This decrease in branching has been proposed to occur through the inhibition of Arp2/3-mediated actin filament branching (Skoble, et al. 2001). The activity of protecting the barbed ends was enhanced by profilin, which required interactions with both VASP, as well as G-actin (Barzik, et al. 2005). VASP has thus been identified as a negative regulator of cell motility, which it does by controlling the geometry of the actin filament networks (Bear, et al. 2002).

1.5. VASP/Vinculin interactions

An interaction between VASP and vinculin was first observed in 1996 by two groups using purified proteins (Brindle, et al. 1996; Reinhard, et al. 1996). The central proline-rich domain in vinculin was found to have an FP_4 motif similar to that found in ActA, and as both VASP and vinculin were known to localize to focal adhesions, it seemed likely that an interaction between the two could exist. Using full-length VASP and vinculin deletion constructs, the interaction site was narrowed down to the central proline-rich region of vinculin, as was expected (Brindle, et al. 1996). At that time, it was unknown which domain of VASP was binding the FP_4 motif. Interestingly, when the C-terminal EVH2 domain was removed, no interaction was detected, and it was postulated that the binding directly involved the EVH2 domain (Brindle, et al. 1996). It is now clear that the EVH1 domain is solely responsible for interaction with the FP_4 motif (Gertler, et al. 1996). Soon after the interaction between VASP and vinculin was discovered, Huttlemaier et al. found that the interaction was enhanced by phosphatidyl-4,5-bisphosphate (PIP_2) (Huttelmaier, et al. 1998). They also postulated from their results that both the EVH1 and EVH2 domains were involved in the interaction, as the other groups had, which as explained above is not the case.

Since these initial three discoveries, no further research has been published on the VASP-vinculin interaction, until 2005, when the interaction between VASP and vinculin was identified in a study involving the "interactome". This was a large-scale yeast two hybrid study with the aim of identifying protein-protein interactions in the human genome, and involved over 8,000 open reading frames (Rual, et al. 2005). Over 80 putative ligands were identified for the vinculin gene, one of which was VASP, which coupled with the previous results, implies that an interaction does in fact occur in cells between the two proteins.

1.6. Purpose of thesis

A sequence analysis of the metavinculin insert by Dr. Eric Ball identified a second, putative VASP binding site in the form of Phe-Pro-Val-Pro-Pro (FPVPP). Based on mutational studies performed using peptides known to bind to VASP (see above), this second site appeared to be a reasonable VASP binding site, as binding was not eliminated when the second proline in the motif was mutated to many of the other amino acids, one of which was valine (Ball, et al. 2000). On the other hand, the motif is not well conserved among pig, chicken, mouse and frog metavinculin sequences. Unlike the human sequence, the residues found in the above species motifs' would most likely eliminate any binding with VASP. The phenylalanine is the only constant residue between the various sequences. If this site in the human metavinculin insert is indeed a second VASP binding site, it might explain why metavinculin is important in cardiac tissue. With metavinculin and VASP both being identified with DCM, this new binding site could shed some light onto the progression of the disease, and perhaps a more appropriate method of treatment.

The ActA protein, which has multiple binding motifs, has a much higher affinity for the VASP protein than vinculin, with its single known site (Machner, et al. 2001). The presence of two sites in metavinculin would be expected to have more than simply an additive effect on the strength of the binding interaction, as is seen with ActA.

Therefore, the goal of this study is to test the hypothesis that the putative binding site identified in the metavinculin insert acts as a VASP binding site, and if so, to identify any differences that may exist between itself and the site found in vinculin. It is hypothesized that the second site is indeed a VASP binding site, and has a similar affinity as that of the known, vinculin site. With the two sites present, the binding is hypothesized to be greatly increased over that of the vinculin site on its own.

CHAPTER 2

EXPERIMENTAL PROCEDURES

2.1. Cloning and Site-directed Mutagenesis

Standard procedures for DNA manipulation were followed (Sambrook, Fritsch and Maniatis 1989).

2.1.1. Metavinculin C-terminal constructs

All Vt and mVt sequences are of human origin. In order to examine the functionality of both the known (site 1) and putative (site 2) VASP binding sites in the mVt, a construct first had to be made which contained both of these sites. To ensure that site 1, which starts at amino acid 842, would be fully intact in our purified protein, a construct starting at amino acid 833 was made (mVt(833-1134)), (Figure 2.1). To accomplish this, two previously constructed plasmids were employed, the first being Vt (833-1066) in the pGEX-KG (Guan and Dixon 1991), and the second being mVt (877-1134), also in pGEX-KG. Both of these constructs have a 5' *EcoRI* site and a 3' *XhoI* site. One fragment was excised from Vt (833-1066) using the 5' *EcoRI* restriction site, and an internal *EarI* restriction site, which cleaves between amino acids 882 and 883. The other fragment was cleaved from mVt (877-1134) using the same internal *EarI* site and the 3' *XhoI* site. These two fragments were ligated together and cloned into pBS-KS+ (Stratagene, Cedar Creek, Texas) to give our new construct spanning from 833 to 1134. This construct was then subcloned into a few different vectors: pEBT7 vector (a modified pET vector encoding a tobacco etch virus (TEV) cleavage site), (Novagen, Madison,

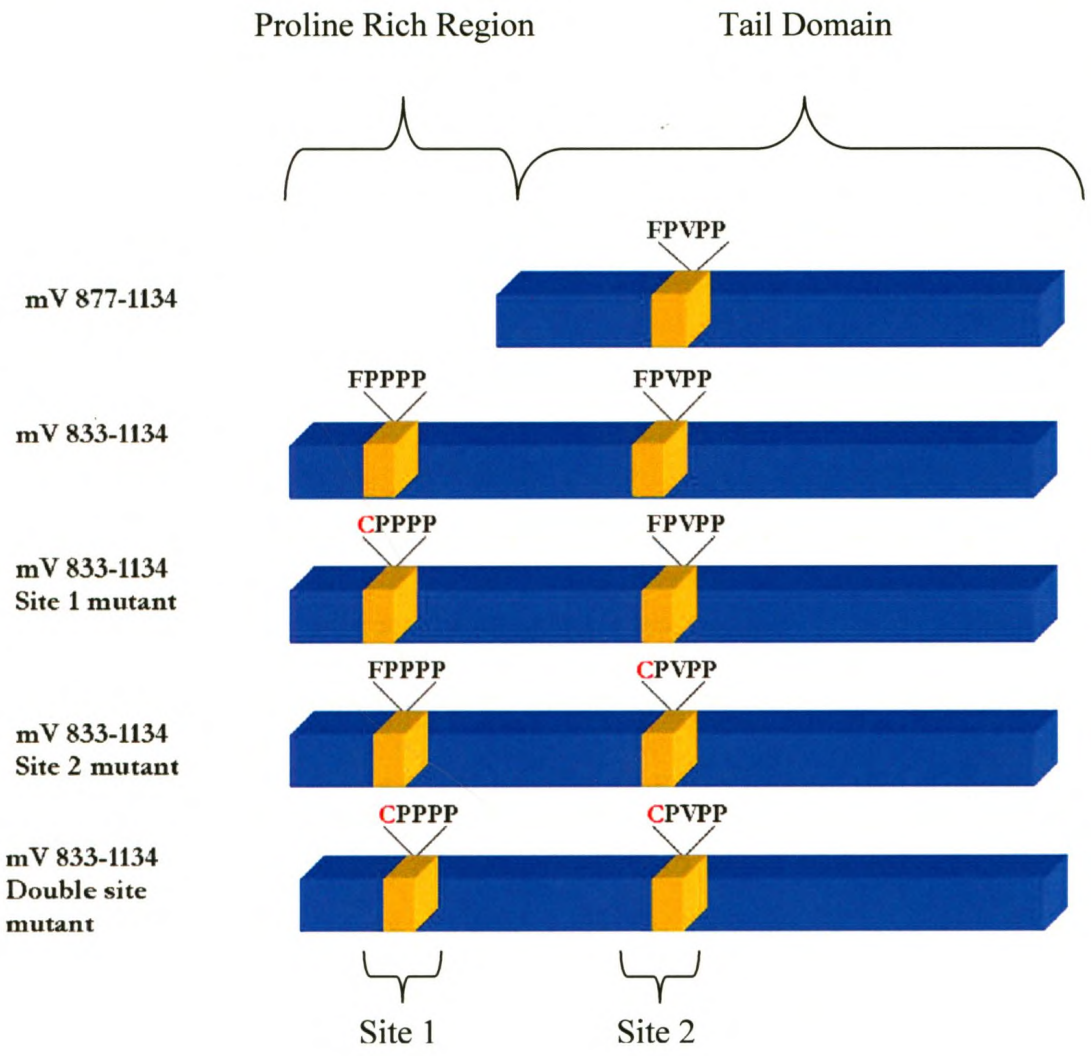

Figure 2.1: mVt constructs. EVH1 binding sites are depicted in gold, with mutated residues shown in red. Mutants were made using a modified megaprimer PCR method.

WI)), a modified pGEX-KG (KG) vector, also encoding a TEV cleavage site (pGEX-KGT), as well as into a pEGFP-C2 vector (Clontech, Mountain View, CA). To clone into this last vector, the construct first had to be cloned into the pEB-T1 vector (Novagen) using the 5' *EcoRI* and 3' *XhoI* sites, from which it was removed using *BamHI* and *XhoI* then ligated into the pEGFP-C2 vector via *BglII* and *SalI* sites, which are compatible with *BamHI* and *XhoI*, respectively. This extra step was required to place the sequence in frame with the GFP.

2.1.2. Binding site mutations

To construct the cysteine mutations in the known (site 1) and putative (site 2) binding sites of the mVt, site-directed mutagenesis was carried out using a modified megaprimer PCR method (Colosimo, et al. 1999), with primers 1 and 2 (Table 1). Phenylalanine 842 and 939 were each mutated to cysteines to form two different mutants; a site 1 mutant, and a site 2 mutant (Figure 2.1), both of which were subsequently cloned into the pEB-T7 vector using *EcoRI* and *XhoI* sites. The mVt833 double site mutant (mVt-DS) was constructed by subcloning with our two new mutants using an internal *AvrII* site, between amino acids 873 and 874. The mutated site 1 was excised from the site 1 mutant using the 5' *EcoRI* site and the *AvrII* site, while the mutated site 2 was excised from the site 2 mutant using the *AvrII* site and the 3' *XhoI* site. These two fragments were ligated together directly into the pEB-T7 vector.

Table 2.1: Oligonucleotide primers used in PCR of various metavinculin and VASP constructs. Consecutive underlined bases denote restriction sites, while single underlined bases denote mutated bases.

Primer #	**Primer Sequence**	**Description**
1	GGGGACAGGGCAACCTGCAGCATCGGC	mVt 833 – F939C (site 2)
2	TGGAGGCGGCGGGCAGTCAGGCTCCTGAGG	mVt 833 – F842C (site 1)
3	GAATTCTAATGAGCGAGACGGTCATC	Forward VASP, *EcoRI* site
4	GCATATGAGCGAGACGGTCATC	Forward VASP, *NdeI* site
5	CTCGAGTCAGGGAGAACCCCGCTT	Reverse VASP, *XhoI* site
6	CAGGACCTCCCCCTCCTCCA	Middle VASP oligo
7	CTCGAGCGGGACCGACCAG	Reverse EVH1 (1-130), *XhoI* site
8	ACTCGAGTTATCCTTCCAACGC	Reverse EVH1 (1-115), *XhoI* site
9	CTCGAGTAGCAACGCCTCTAGGGCACT	Reverse EVH1 (1-113), *XhoI* site

2.1.3. VASP plasmids

The human VASP clone was obtained from MGC, clone 40541(ATCC, Manassas, VA). Four different constructs of the EVH1 domain were made using PCR (Figure 2.2). The first construct, made using primers 3 and 9 (Table 1), spanned amino acids 1-113; the second construct, made using primers 3 and 7 (Table 1), spanned amino acids 1-130. The third construct, made using primers 3 and 8 (Table 1), and the fourth construct, made using primers 4 and 8 (Table 1), spanned amino acids 1-115, which encompasses the entire EVH1 domain, with the former having an *EcoRI* site, and the latter having a *NdeI* site at the 5' end. All of the constructs were ligated into the pEB-T7 vector, and construct three was also ligated into the KG-T vector.

After some initial difficulty with PCR to obtain full-length VASP sequence, a different approach was taken in which 3 smaller segments were separately cloned. The first 109 base pairs were taken from the EVH1 (1-113) construct, using an internal *BglII* site, and the *EcoRI* site put in with primer 3 (Table 1). The middle segment, spanning from base pair 109 to 588, was taken from the VASP plasmid using the above *BglII* site and an internal *PstI* site. The third segment, spanning from base pair 520 to 1143, was made using primer 5 and 6 (Table 1). This third segment was ligated into pCR-blunt (Invitrogen, Carlsbad, CA), and digested out using *PstI* and *XhoI*, the latter of which was put in with primer 5 (Table 1). Segments 1 and 2 were first ligated together into pBS-KS+ cut with *EcoRI* and *PstI*, creating an N-terminal segment spanning *EcoRI* to *PstI*. This was the ligated together with the C-terminal segment, and inserted into the pEB-T7 vector. The full-length VASP construct was also ligated into a pCDNA3.1(+) vector (Invitrogen), using the *EcoRI* and *XhoI* sites.

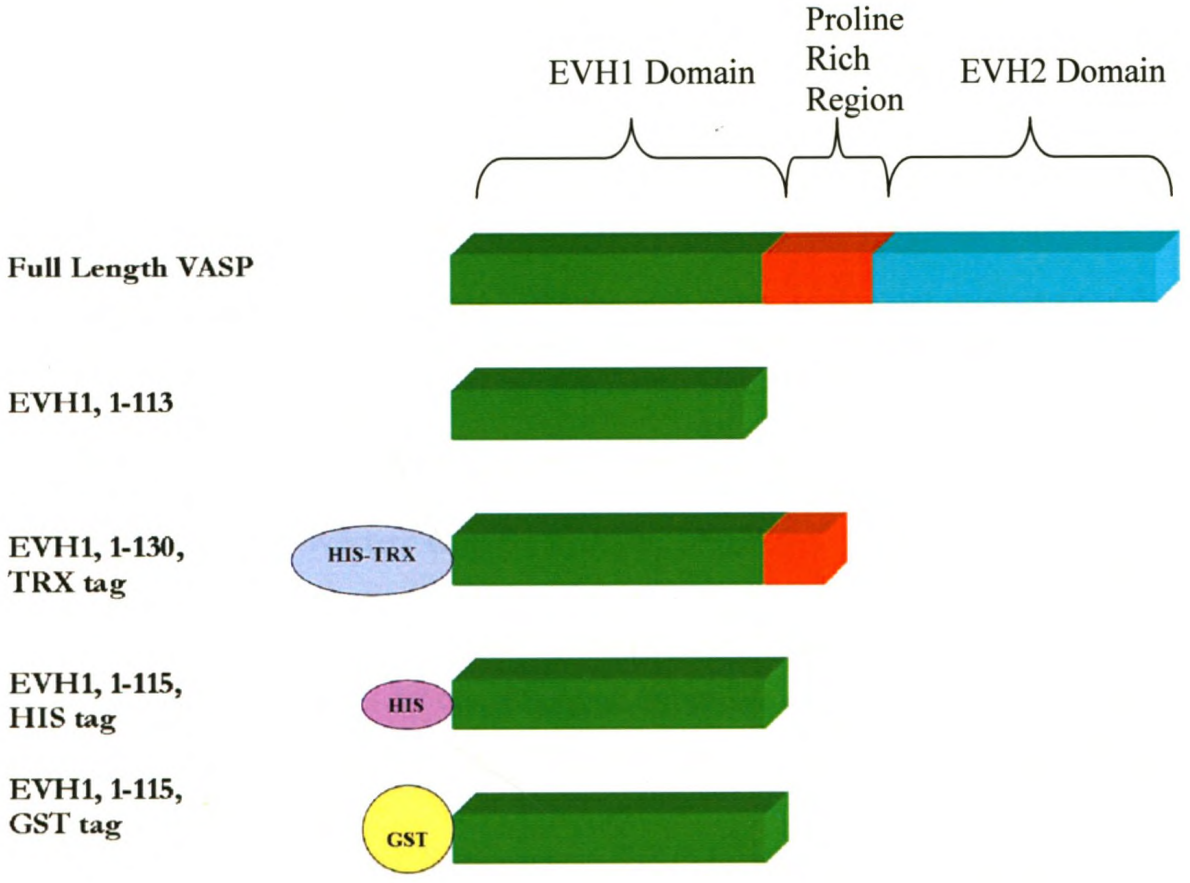

Figure 2.2: VASP constructs. The EVH1 domain is depicted in green, the proline rich region in red and the EVH2 domain in teal.

2.1.4. Other plasmids

Previous lab members and Dr. E. Ball had constructed many of the plasmids used. These included Vt833 in the pEB-T2 vector and Vt877-buried cysteine mutant (C950T, C972A, T1037C) in the pEB-T7, the mVt877 in the pEB-T7 vector, Cf Vt877 (C950T, C972A, C985S), a cysteine-free version of Vt in pEB-T7. Vt877 (P878C) was constructed and the protein purified by Courtney Voss, a current student in the lab.

All PCR products were cloned into the pCR-Blunt vector and sequenced at the Robarts sequencing facility (University of Western Ontario, London, ON). All primers were designed using GeneRunner, v.3.05, and were purchased from the UWO Oligo Factory (University of Western Ontario, London, ON).

All the constructs were transformed into BL21 (DE3) *Escherichia coli* cells for protein expression. The pEB-T7 constructs are expressed as either a thioredoxin plus his-tag fusion (*EcoRI* site) or a hexa-histidine fusion (*NdeI* site). The KG and KG-T constructs produce glutathione-S-transferase (GST) fusions. In addition, proteins cleaved from KG-T contained fewer additional amino acids from the vector at their N-terminus; cleavage from KG-T results in the addition of GSPGILE while cleavage from KG results in the addition of SPGISGGGGGILE.

2.2. Protein Expression and Purification

2.2.1. Thioredoxin fusions

Stocks were streaked on agar plates and approximately 10 colonies were added to 100mL of M9 medium containing 0.4% glucose, 0.2% casamino acids, and100μg/mL ampicillin, which was then shaken overnight at 37°C. This was diluted into 1L of LB medium containing 100μg/mL ampicillin, and continued shaking at 37°C for two more

hours, at which point the cells were treated with 0.2mM IPTG. The cells were left to grow at room temperature for four more hours then centrifuged at 3,000 x g for 10 minutes and resuspended in TE (10mM Tris-HCl, pH 8.0, 1mM EDTA). Protease inhibitors were added to the cell suspension (0.2mM PMSF, 2μg/mL leupeptin, 5mM EDTA), and it was passed through a french pressure cell at 20,000 p.s.i. or through an Emulsiflex-C3 cell homogenizer (Avestin, Ottawa, ON). The lysate was centrifuged for one hour at 100,000 x g, 4°C, to remove cellular debris.

EVH1 constructs

The supernatant from the previous step was passed through a 10ml DEAE column (GE Healthcare) at 4°C, and the flow-through saved. Prior to loading onto a 5mL Ni-NTA column (Qiagen, Valencia, CA), imidazole to 10mM and $CaCl_2$ to 1mM were added to the sample. The column was then washed with 10 column volumes of TNM-300 (10mM Tris-HCl, pH 7.5, 300mM NaCl, 5mM β-ME) containing 10mM imidazole. EVH1 protein was eluted with TNM-300 containing 250mM imidazole, followed by the immediate addition of EDTA to 1mM to the protein fractions. The final proteins had percent purities ranging from 79 to 90%, with average yields of 0.7mg/L of culture.

Metavinculin/vinculin constructs

The supernatant was passed through a 10ml S-Sepharose column (GE Healthcare) at 4°C, and the column washed with 10 column volumes of TEM (10mM Tris-HCl, pH 7.5, 1mM EDTA, 5mM β-ME) containing 10mM NaCl. Vinculin, or metavinculin, tail domain was eluted with TEM containing 400mM NaCl. Prior to loading onto a 5mL Ni-NTA column, imidazole to 10mM and $CaCl_2$ to 1mM were added to the sample. After

loading, the column was washed with 10 column volumes of TNM-300 containing 10mM imidazole. Protein was eluted with TNM-300 containing 250mM imidazole and EDTA to 1mM was immediately added to the protein fractions. The thioredoxin tag was cleaved off by treatment with 20μg TEV/mg protein at room temperature overnight while dialyzing into TEM containing 50mM NaCl. To further purify and concentrate the protein, a 1mL S-sepharose column was employed. After loading the sample, the column was washed with 5 column volumes of TEM containing 50mM NaCl, followed by elution with TEM containing 300mM NaCl. Purification of mVt is shown in Figure 2.3, with the final purified protein having a purity of 70%, and an average yield of 2mg/L of culture. This was similar for the mutants, with purity ranging between 75 and 85%, and yields of the same amount as wild-type. Vt833 in T2 was purified in the same manner, except thrombin was used to cleave the fusion.

2.2.2. GST fusions

EVH1 construct

The cells were expressed and induced as described above and the supernatant run through a 5mL glutathione-agarose column (Sigma, St. Louis, MO). The column was washed with 10 column volumes of TBS containing 1mM EDTA and 5mM β-ME. The protein was eluted with TBS, 1mM EDTA, 5mM β-ME, and 5mM glutathione. Before further purifying and concentrating on a 1 mL DEAE column, the sample was diluted with an equal volume of dH_2O to decrease the salt concentration. After loading the

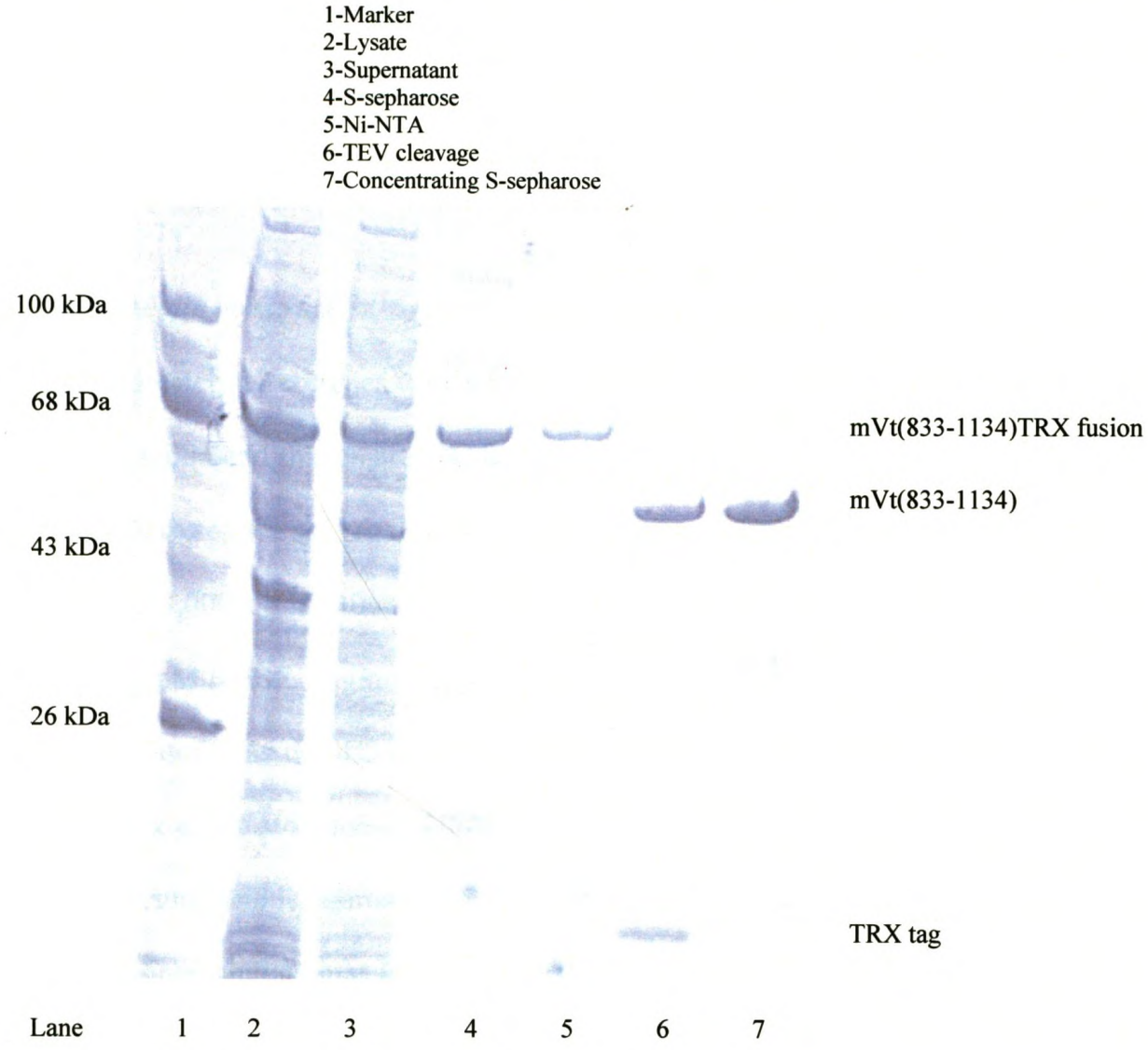

Figure 2.3: Purification of mVt (833-1134). SDS-PAGE of samples from different stages of purification. Lanes 4 to 7 contain ~1μg of protein. Percent purity of final product in lane 7 is ~70%. Gel is stained with Coomassie stain.

sample, the column was washed with 5 column volumes of TEM containing 70mM NaCl, and the protein was eluted using TEM containing 300mM NaCl. The purification is shown in Figure 2.4, with the final purified protein having a purity of 79% and an average yield of 6mg/L of culture.

Metavinculin construct

Approximately 12 colonies were added to 1L of TB medium containing 100μg/mL ampicillin and shaken at 37°C for six hours, at which point 0.2mM IPTG was added. The cells were then shaken overnight at room temperature, pelleted by centrifugation at 3,000 x g for 10 minutes and resuspended in TBS. Protease inhibitors were added (0.2mM PMSF, 2μg/mL leupeptin, 5mM EDTA), and the cells lysed by passing through an Emulsiflex-C3 cell homogenizer. The lysate was centrifuged for one hour at 100,000 x g, 4°C, to remove cellular debris. The supernatant was then passed through a 10mL glutathione-agarose column, and the column washed with 10 column volumes of TBS containing 5mM β-ME. The protein was eluted with 5mM glutathione in TBS, 5mM β-ME. Before further purifying and concentrating on an S-sepharose column, the sample was diluted with one volume of dH_2O to decrease the salt concentration. The column was washed with 5 column volumes of TEM containing 70mM NaCl. The protein was eluted using TEM containing 300mM NaCl. The final protein had a purity of 80%, with an average yield of 1mg/L of culture.

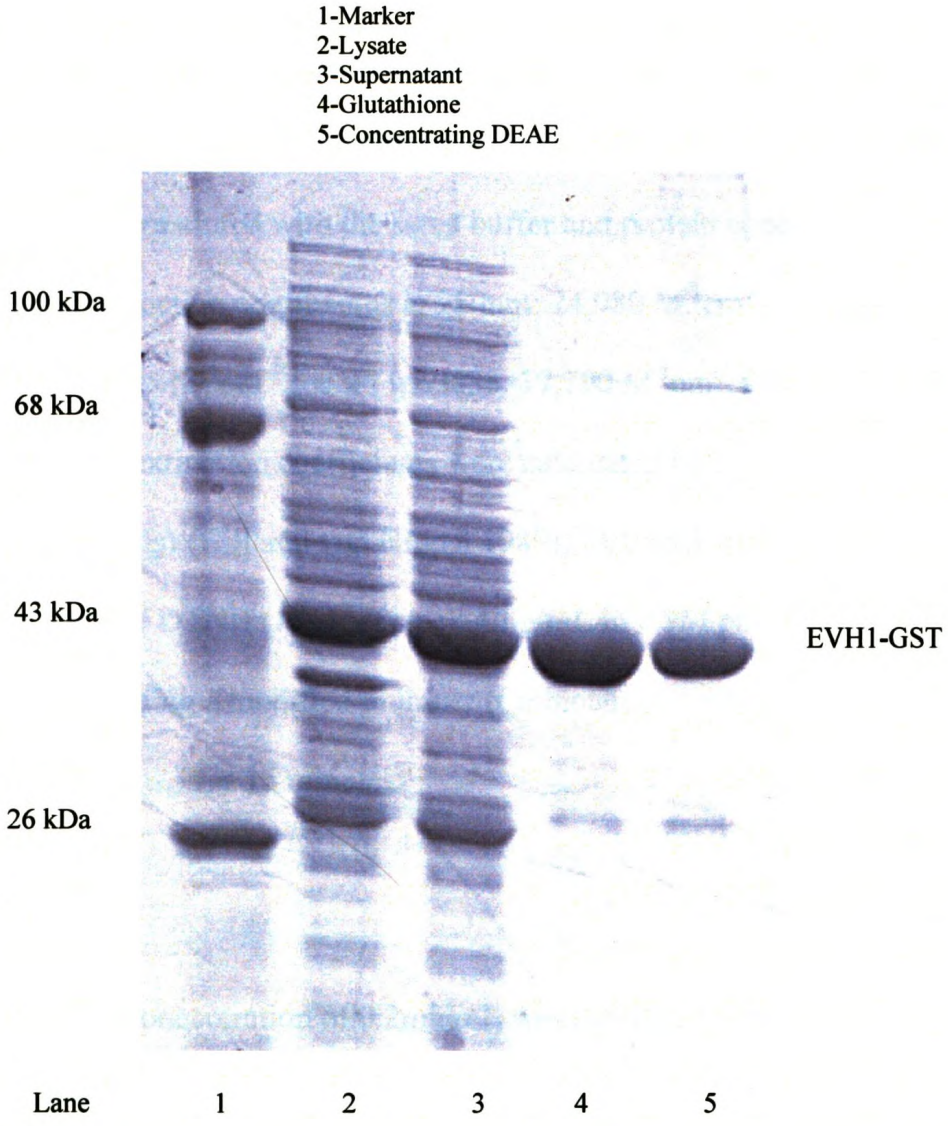

Figure 2.4: Purification of EVH1-GST. SDS-PAGE of samples from purification of EVH1 (1-115)-GST. Lanes 4 and 5 contain ~9μg of protein. Percent purity of final product in lane 5 is ~79%. Gel is stained with Coomassie stain.

2.3. DTNB Assay

Protein samples were reduced with 2mM DTT at room temperature for 30 minutes. Excess DTT was removed from the sample by gel filtration on a 10mL P6 column (Bio-Rad, Hercules, CA) equilibrated with 0.1M phosphate, pH 8.0 and 1mM EDTA. Fractions were eluted with the same buffer and protein concentration determined using calculated extinction coefficients at 280nm: 24,980 $M^{-1}cm^{-1}$ for mVt833-Cf, site 1 and 2 mutants, 25,105 $M^{-1}cm^{-1}$ for Wt mVt833, 17,790 $M^{-1}cm^{-1}$ for Vt877-P878C and Vt877-buried sites (extinction coefficients were calculated by ExPASy ProtParam tool www.expasy.org/tools) (Gill and von Hippel 1989)). A 0.6mL volume at 1mg/mL was made up and 40µg of DTNB (10µL of stock 4mg/mL in 0.1M phosphate, pH 8.0, 1mM EDTA) was added using a modified plumper (Calbiochem, La Jolla, CA). The reaction was monitored at OD_{412} for 15 minutes.

2.4. Gel Filtration

Protein at a concentration of 0.2mg/mL was incubated for 15 minutes at room temperature, followed by centrifugation at 350,000 x g for 12 minutes at 4°C. The supernatant was loaded onto a 24mL Superose-12 column (GE Healthcare), and was eluted at 0.5mL/minute with TE containing 100mM NaCl and 0.5mM DTT. Two minute fractions were collected, of 1ml volumes and samples analyzed on 12% SDS-PAGE.

2.5. GST and Nickel Pull-downs

Proteins were incubated together for fifteen minutes at room temperature before an equal volume of 50% bead slurry (glutathione-agarose in TBS or Ni-NTA agarose in TNM-100 (10mM Tris-HCl, pH 7.5, 100mM NaCl, 5mM β-ME) containing 10mM

imidazole) was added. The samples were rotated for twenty minutes at room temperature, and then briefly centrifuged (3 seconds in microfuge). The supernatant was aspirated, the beads were washed with the respective buffer and resuspended in Laemmli sample buffer with 5mM glutathione or 250mM imidazole to elute the bound proteins.

When lipids were used, they were added before the addition of the bead slurry and incubated for fifteen minutes with the proteins at room temperature. Lipids used were PI (1mM), (Sigma), and PIP_2 (120μm), (Avanti Polar Lipids, Alabaster, AL).

2.6. Actin Binding

Actin binding was detected using a method similar to that of Hemmings *et al.* (1996). mVt and EVH1-GST (0.1mg/mL) were first mixed together in 10mM Tris-HCl, pH 8.0, 0.2mM ATP, 0.2mM $CaCl_2$ and 0.02% Triton X-100. G-actin (0.2mg/mL) (Cytoskeleton, Denver, CO), in 10mM Tris-HCl, pH 8.0, 0.2mM ATP, 0.2mM $CaCl_2$, 5% (w/v) sucrose and 1% (w/v) dextran, was added, followed by 100mM NaCl and 1mM $MgSO_4$ to polymerize the actin. After incubation at room temperature for one hour the sample was centrifuged at 90,000 x g, 25°C for one hour. Pellets were carefully washed with PBS, and resuspended in an equal volume of PBS. Samples of supernatant and pellet were mixed with Laemmli sample buffer and analyzed by 15% SDS-PAGE.

2.7. Labeling of Mutants

2.7.1. FITC (fluorescein isothiocyanate)

The purified mVt protein (0.5mL of 3.3mg/mL) was first dialyzed into PBS, 1mM EDTA for six hours, and ¼ volume of 1M $NaHCO_3$, pH 8.5 was added. FITC (Research Organics Inc, Cleveland, OH) (10mg/mL in DMSO) was added to give 200μg FITC/mg

protein, and subsequently left in the dark at room temperature for two hours. The protein was dialyzed into TEM with 5mM NaCl, and was further purified and concentrated on a 1mL S-sepharose column. The extent of labeling was estimated from absorbance at 493nm.

2.7.2. CPM (7-diethylamino-3-(4'-maleimidyl-phenyl)-4-methylcoumarin)/NPM (N-(1-pyrenyl) maleimide)

The purified protein (either site 1 or site 2 mutants – 0.5mL of 5mg/mL) was reduced with 2mM DTT at room temperature for thirty minutes, before DTT was removed by passing the sample through a 10mL P6 column equilibrated in 0.1M phosphate, pH 8.0, 1mM EDTA. Fractions were eluted with the same buffer and protein concentration determined using OD_{280} (extinction coefficient 24,980 $M^{-1}cm^{-1}$) The reduced protein at a concentration of ~1mg/mL, was mixed with 10μL of CPM (Invitrogen) or NPM (Sigma), (16mg/mL in DMF), and left at room temperature in the dark for two hours. The protein was then dialyzed into TEN-50 overnight at 4°C. The protein was further purified and concentrated by passing through a 1mL S-sepharose column, and the extent of labeling determined from absorbance at 338nm for CPM or 387nm for NPM.

2.7.3 Biotin

The purified mVt site 1 or site 2 mutants were first reduced with 2mM DTT at room temperature for thirty minutes and DTT removed on a P6 column as above. The reduced protein at a concentration of ~1mg/mL in 1mL, was mixed with 50μL of N-iodoacetyl-N-biotinylhexylenediamine (Pierce, Rockford, IL), or 10μL of biotin-

maleimide (Sigma), both 2mg/mL in DMF, and left at room temperature in the dark for two hours. The protein was then dialyzed into TEN-50 overnight at 4°C.

2.8. Fluorescence Subtraction Assay

FITC labeled mVt plus unlabeled EVH1-GST were mixed together and incubated for 30 minutes at room temperature, then an equal volume of 50% bead slurry (glutathione-agarose in TBS) was added to the reaction, followed by rotation for one hour at room temperature. The samples were centrifuged (20 seconds in microfuge), and supernatants removed and saved. To ensure all of the GST-fusion protein had been removed from the supernatant, a portion was run on a 12% SDS-PAGE gel. The remaining supernatants were then assayed on a FluoroLog-3 fluorimeter (Horiba Jobin Yvon, Edison, NJ) equipped with a thermoregulated sample compartment (21°C). All samples were first centrifuged at 350,000 x g for 10 minutes, 4°C. FITC was excited at 493 nm and peak emission was monitored at 518 nm, with slit widths of 2.0 nm, at five second intervals for a total time of 3600 seconds. The buffer used was TE containing 100mM NaCl and 1mg/mL BSA.

2.9. Fluorescence Perturbation Assay

This assay was performed using a FluoroLog-3 fluorimeter as above. The total reaction volume was 3mL, with TE containing 100mM NaCl added to the cuvette initially, followed by BSA to 1mg/mL. Once a stable baseline was established with the buffer + BSA, the fluorescently labeled mVt was added, up to a concentration of 0.1μM. EVH1-GST was added once a stable signal was established with the fluorescent mVt, to a final concentration of 13.7μM. CPM was excited at 384 nm and peak emission was

monitored at 469 nm, while NPM was excited at 338 nm and peak emission was monitored at 375 nm, both with slit widths of 2.0 nm, at five second intervals for a total time of 3600 seconds.

2.10. Transfections/Immunoprecipitates

Plasmid DNA from mVt833-pEGFP-C2 and VASP-pCDNA3.1(+) was prepared to give a final concentration of 40μg of DNA/10cm plate. As a positive control, 7μg pEGFP/10cm plate was also prepared. The cells used were U2OS (human bone osteosarcoma epithelial), and were seeded by Ashley Bibby of Dr. Litchfield's lab. Calcium phosphate coprecipitation of DNA was used for transfection of cells (Ausubel, et al. 1990), and subsequently left for sixteen hours at 37°C/5% CO_2, at which point the precipitate was washed off the cells. The cells were then left for twenty-four hours for protein expression. The cells were harvested using lysis buffer (50mM Tris-HCl, pH 7.5, 150mM NaCl, 1% NP-40) followed by sonication, and a spin to clear the samples.

To the cell lysates, 2μg of anti-GFP (Invitrogen) was added, and incubated at 4°C for thirty minutes. 14μL of protein A-agarose (GE Healthcare) in PBS was added to each sample and further incubated at 4°C for thirty minutes. The samples were briefly microfuged (3 seconds) and the supernatants were transferred to fresh tubes. After 4 washes with 1mL of Triton X-100 lysis buffer (50mM Tris-HCl, pH 7.5, 150mM NaCl, 1% Triton X-100), Laemmli sample buffer was added, the samples boiled, briefly microfuged, and the eluate electrophoresed on 12% SDS-PAGE.

2.11. Western/Far Western Blots

2.11.1. Western blots

Gels were equilibrated in Blot running buffer (48mM Tris, 39mM Glycine, 0.037% SDS, 20% MeOH) for 15 minutes, and protein then electrophoretically transferred onto an Immobilon-P (PVDF) membrane (Millipore, Billerica, MA) at 100V for one hour. After the transfer, the proteins were visualized with 0.0025% amido black in 50% MeOH and 10% glacial acetic acid, and marked with a ball point pen. After blocking the membrane with 5% skim milk in TBS, it was probed with anti-VASP (BD Biosciences, Franklin Lakes, NJ), at a concentration of 500 ng/mL in TBS/5% skim milk and 0.02% sodium azide at room temperature overnight, followed by a three hour probe with alkaline phosphatase-conjugated goat anti-mouse IgG (GE Healthcare), at a concentration of 200 ng/mL in TBS/5% skim milk at room temperature. The blot was developed as follows: 33µL of NBT was mixed with 10mL alkaline phosphatase buffer (100mM NaCl, 5mM $MgCl_2$ and 100mM Tris, pH 9.5), followed by 16.5µL BCIP. This solution was added to the membrane and developed at room temperature until desired bands were visible.

2.11.2. Far Western blots

Protein samples were electrophoresed and transferred to a nitrocellulose membrane as above. Following blocking with 3%BSA in TBS, binding to EVH1-GST was done at a concentration of 500 ng/mL in TBS/3% BSA overnight at room temperature, followed by probing with monoclonal anti-GST (WITS, London, ON), at a concentration of 250 ng/mL in TBS/3% BSA for two hours. The membrane was probed with alkaline phosphatase-labeled goat anti-mouse IgG, at a concentration of 200 ng/mL

in TBS/3% BSA for two hours. The blot was developed using NBT and BCIP in alkaline phosphatase buffer for 20 minutes, at which point the bands were visible.

2.12. Nitrocellulose Binding Assays

The desired proteins were dotted in a volume of 1μL onto 1.0 x 10cm strips of nitrocellulose membrane, and allowed to dry for fifteen minutes. The blots were blocked for two hours in TBS with either 3% BSA or 5% skim milk, and then washed twice for ten minutes each with TBS. All of the binding and probing was done in 1XTBS with either 3% BSA or 5% skim milk at room temperature. The binding with the GST labeled protein was at a concentration of 500 ng/mL for two hours, followed by two 10 minute washes with TBS. The blots were then probed with monoclonal anti-GST at a concentration of 250 ng/mL for two hours, followed by two, 10 minute washes with TBS, and a final probe with alkaline phosphatase-labeled goat anti-mouse IgG, at a concentration of 200 ng/mL. The blots were washed twice more for ten minutes with TBS, and developed using NBT and BCIP in alkaline phosphatase buffer. The development of the blots was monitored closely, and was stopped by removing the solution and rinsing the blots in ddH_2O. The visualized spots on the blots were then analyzed using an AlphaImager, and the spot densitometry function of the AlphaEase imaging software (Alpha Innotech, San Leandro, CA).

To detect the biotin-labeling of the mVt, the protein was dotted on to the blots and probed with alkaline phosphatase conjugated to streptavidin (Jackson ImmunoResearch Laboratories, West Grove, PA).

After conditions had been explored, the assay was standardized as follows: each blot had BSA (1μg), GST (20ng), mVt (1μg), mVt (500ng) and mVt (100ng) as

standards; all blocking, binding and probing buffers contained 5% skim milk; all blots were left overnight with the monoclonal anti-GST antibody, and all blots were developed for 15 minutes.

For the blots where the NaCl concentration was modified from the standard TBS, the modified buffer was 20mM Tris, pH 7.5 and a range of NaCl concentrations between 5mM and 500mM. This modified buffer was used for the entire assay.

For the blots where the pH was modified from the standard of 7.5, the modified buffer was 20mM Tris, with pH of 6.0, 8.0 or 9.5, with the standard NaCl concentration of 140mM. This modified buffer was used only for the first half of the assay, up until after the washes after binding. At this point the blots were fixed in 2mL of formaldehyde in PBS for 5 minutes, followed by two 10 minute washes with TBS. The remainder of the assay was performed as above.

For the blots with the lipids, the proteins were first incubated for 30 minutes at 37°C with PI, and were then dotted onto the membrane. The assay was performed as above.

For the blots with EDTA with and without $CaCl_2$, the modified buffers, containing 1mM EDTA ± 1mM $CaCl_2$, were used for the entire assay.

2.13. Other Techniques

Protein concentrations were determined by the method of Lowry (Lowry, et al. 1951) as modified by Peterson (Peterson 1977) unless otherwise stated. SDS-PAGE was carried out using the Laemmli buffer system (Laemmli 1970) and the protein standard molecular weights are shown in kDa.

CHAPTER 3

RESULTS

3.1. Protein Expression

Based on a sequence analysis done by Dr. Eric Ball, a second putative VASP binding site motif was identified in the metavinculin insert, in the form of FPVPP. From previous mutational analysis of each residue involved in the consensus motif, it is known that the phenylalanine is essential, with the exception of being replaced with either a tryptophan, lysine or tyrosine (Ball, et al. 2000). To make mutants in which the binding was knocked out in both the vinculin site (site 1) and the metavinculin site (site 2), the phenylalanine in each site was separately mutated to a cysteine. The mutations did not cause any noticeable protein stability problems in *E.coli*, as the expression levels were comparable with that of the wild-type. The purification was performed identically for the mutants and the wild-type, with the mutants behaving similarly to the wild-type construct, all having a final purified yield of approximately 2mg/L of culture. The mutants, which are in a cysteine free background, were verified to be exactly what they were thought by the DTNB assay, which allowed for the calculation of thiol groups present, with both mutants having one detectable thiol each. The percent purity of the two mutants and the wild-type ranged between 70 and 85% (Figure 3.1, lanes 6, 8 and 9). Other vinculin/metavinculin proteins purified are shown in Figure 3.1, lanes 5, 7, 10-13. All of these proteins are relatively pure, with minimal degradation. The lower bands seen in the metavinculin constructs appeared during storage (Figure 3.1, lanes 5-9).

Full-length VASP proved to be insoluble when expressed in *E.coli*. A number of constructs containing the EVH1 domain were tested, as some stability issues were

1 – Marker
2 – EVH1 (1-115)-His
3 – EVH1 (1-130)-TRX
4 – EVH1 (1-115)-GST
5 – mVt-877
6 – mVt-833(wt)
7 – mVt-833-CF
8 – site 1 mutant (F→C)
9 – site 2 mutant (F→C)
10 – mVt-833-GST
11 – Vt-buried cysteines
12 – Vt-833
13 – mVt-double site mutant

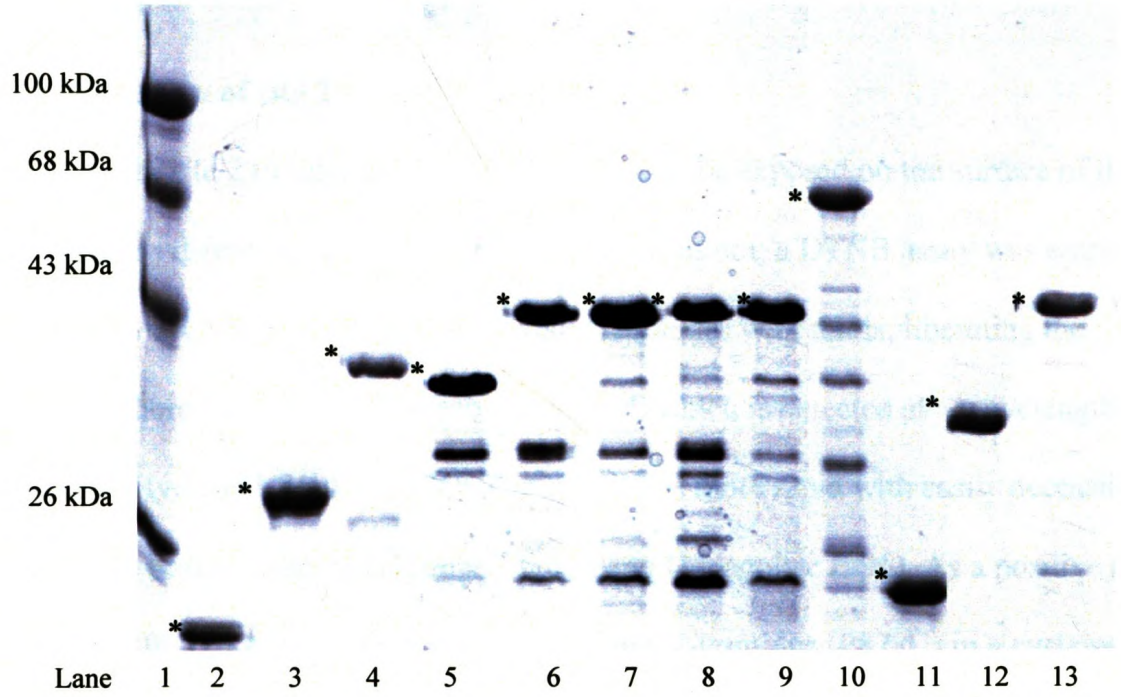

Figure 3.1: 12% SDS-PAGE of purified proteins. EVH1 constructs – lane 2 to 4; metavinculin constructs – lane 5 to 10, 13; vinculin tail constructs – lane 11 and 12. Full-length species are denoted with an *. All lanes contain ~1μg of protein. Gel is stained with Coomassie stain.

encountered. EVH1 (1-113) was rapidly degraded during purification, while EVH1 (1-130)-TRX was slightly more stable, but with low expression (~0.7mg/L of culture) (Figure 3.1, lane 3). EVH1 (1-115)-his was much more stable than the previous two constructs, but expression was still low (~0.7mg/L of culture) (Figure 3.1, lane 2). The final construct, EVH1 (1-115)-GST was the most stable of the constructs and had the highest expression levels (6mg/L of culture), with a percent purity of 79% (Figure 3.1, lane 4).

3.2. Exposure of site 2

For site 2 to interact with VASP, it had to be exposed on the surface of the protein. To determine whether this was the case or not, a DTNB assay was employed, in which the DTNB molecule forms mixed disulphides with thiols, liberating the chromophore 5-mercapto-2-nitrobenzoic acid, which is detected at a wavelength of 412nm (Hyde and Walker 1974). The reaction is more rapid with easily accessible thiols than with buried cysteines (Ramachandran and Udgaonkar 1996). As a positive control, a Vt (878-1066) construct with a cysteine on the N-terminus (P878C) in a cysteine free background, was used. This protein underwent very rapid reaction, which was complete within 5 seconds (Figure 3.2). In contrast, a mutant which contained only two buried cysteines, Vt (C972A, C950T, T1037C) reacted slowly, with absorbance gradually increasing over 15 minutes. The site 1 mutant reacted rapidly, although not quite so quickly as the P878C protein, while a thiol-free protein (mVt-833-CF) showed a small initial rise in absorbance but no further increase. The site 2 mutant reacted rapidly, similar to the P878C rather than the Vt with the buried cysteine, indicating a high degree of exposure.

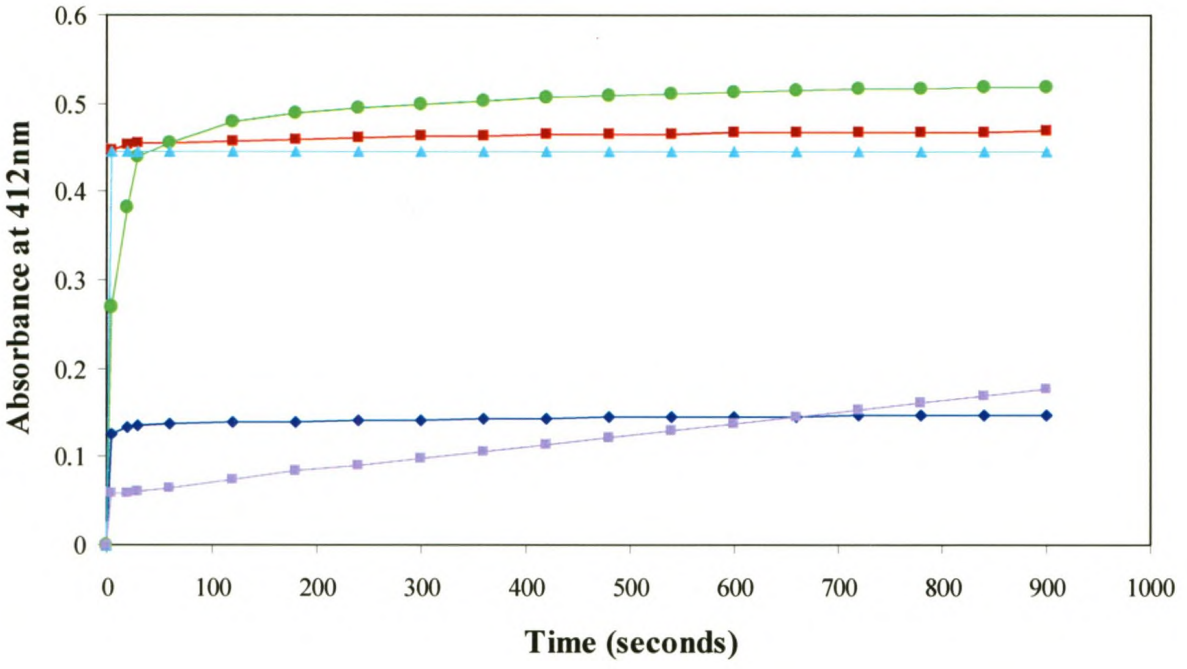

Figure 3.2: Absorbance at 412nm after addition of DTNB. 40µg of DTNB was added to a 1mg/mL sample of each protein and absorbance was monitored at 412nm for 15 minutes. ♦ - mVt833-CF; ■ – site 2 mutant (F->C); ● – site 1 mutant (F->C); ▲ – Vt P878C; ■ – Vt buried cysteines.

3.3. VASP binding to site 1 and 2

In order to study the binding of VASP to site 1 and site 2, a binding assay was first needed. Various methods were tested in the hope of finding a facile, accurate assay.

One of the first binding assays attempted was an FPLC gel filtration assay. This is a simple and convenient method for detecting protein-protein interactions in solution as the formation of a protein complex causes an elution shift (Sheehan 1996). The mVt by itself eluted from a Superose-12 column between 16 and 17 mL (Figure 3.3B, lanes 9 and 10), while the EVH1 (1-130) construct eluted between 17 and 19 mL (Figure 3.3A, lanes 10 to 12). After incubating them together, the EVH1 protein eluted in essentially the same place (Figure 3.3C, lanes 10 to 12), but the mVt did elute one fraction earlier (Figure 3.3C, lanes 8 and 9). Little co-elution was seen, however. Similar results were seen in three separate experiments, all of which suggest a low affinity, but it is unclear as to whether this is the case.

The next assay tried was a nickel pull-down assay, which involved the use of an EVH1 construct with an N-terminal hexa-histidine tag (EVH1-his), which binds to Ni-NTA resin. After incubating the proteins together and adding resin, co-precipitated mVt was visualized on SDS-PAGE. However, the amount of metavinculin that bound to the resin in the absence of EVH1-his was very high and no increase was seen in the presence of EVH1-his (results not shown).

In an attempt to reduce background a similar assay was attempted, a GST pull-down assay, that differed as it involved an EVH1 construct as a GST fusion (EVH1-GST) which binds to glutathione resin. This assay was tested in the presence and absence of lipids, as it has been previously reported that lipids enhance the vinculin-VASP interaction (Huttelmaier, et al. 1998). The glutathione beads brought down a large

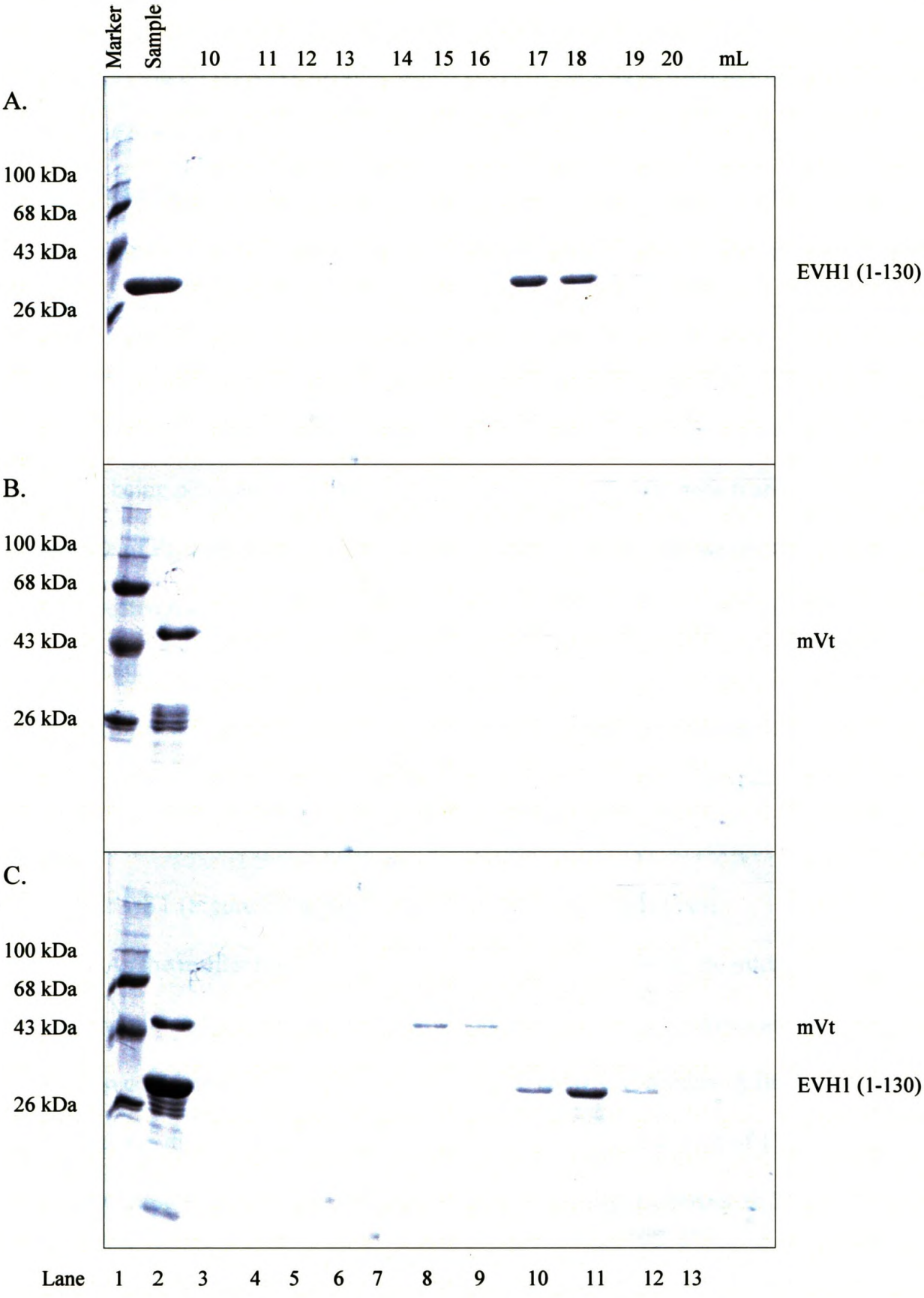

Figure 3.3: 12% SDS-PAGE of gel filtration of mVt with EVH1 (1-130) on a Superose-12 column. A. EVH1(1-130) only. B. mVt only. C. EVH1 + mVt. *n*=3. Gel is stained with Coomassie stain.

amount of the EVH1-GST fusions, which is visible as a large band in Figure 3.4A, lane 2. This lane also shows that no contaminating bands are seen at the same size as mVt, which is shown in Figure 3.4A, lane 3, in the amount present in the assay. In the absence of lipids, when mVt was present with EVH1-GST, only a small amount of mVt was precipitated (Figure 3.4A, lane 4). However, an almost equal amount came down with the GST control (Figure 3.4A, lane 5). In the presence of lipids, a similar result was seen, with a small amount of mVt being precipitated with the EVH1-GST, and a similar amount being precipitated with the GST control (Figure 3.4B, lanes 6 and 5). In the presence of PI, a slight increase is seen (Figure 3.4B, lane 7). However, this experiment was repeated four times, and the increase was not consistent. The PIP_2 and IP_6 showed no effect on the interaction in any of the trials (Figure 3.4B, lanes 8 and 9). This assay was also performed with mVt (877), which contains site 2 only, in the absence of lipids only (Figure 3.4A, lane 6-8). Due to the size similarity between mVt (877) and EVH1-GST, it was difficult to determine if there was a difference in mVt (877) present with EVH1-GST and with GST (Figure 3.4A, lanes 7 and 8), but it was small at best.

As the results from the preceding experiments indicated, the interaction between metavinculin and VASP had a much lower affinity than the pull-down assays or gel filtration could detect, therefore a more sensitive assay was needed. A literature search revealed a method in which low affinity interactions, reaching a Kd of 11.5μM, were detected using a fluorescence supernatant depletion assay (Cohen, et al. 2005). In this assay, mVt-FITC remaining in the supernatant was measured after EVH1-GST was precipitated with glutathione beads. This method had the advantage that no washing steps were required. The mVt protein was labeled with FITC to a molar ratio of 0.14 FITC/mVt. To ensure all of the EVH1-GST protein was pulled down, a portion of the

A.

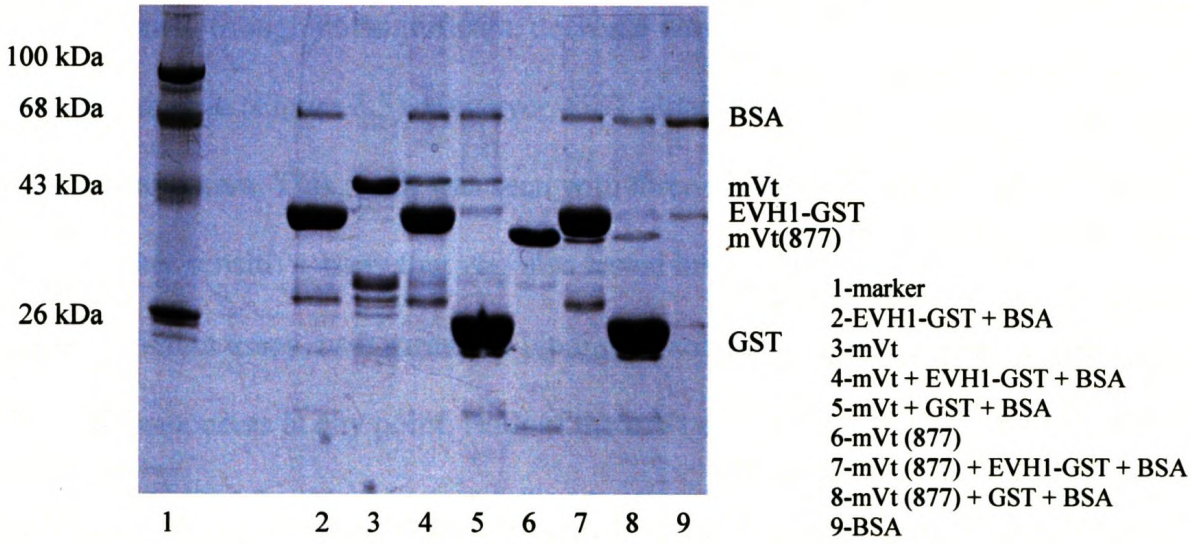

B.

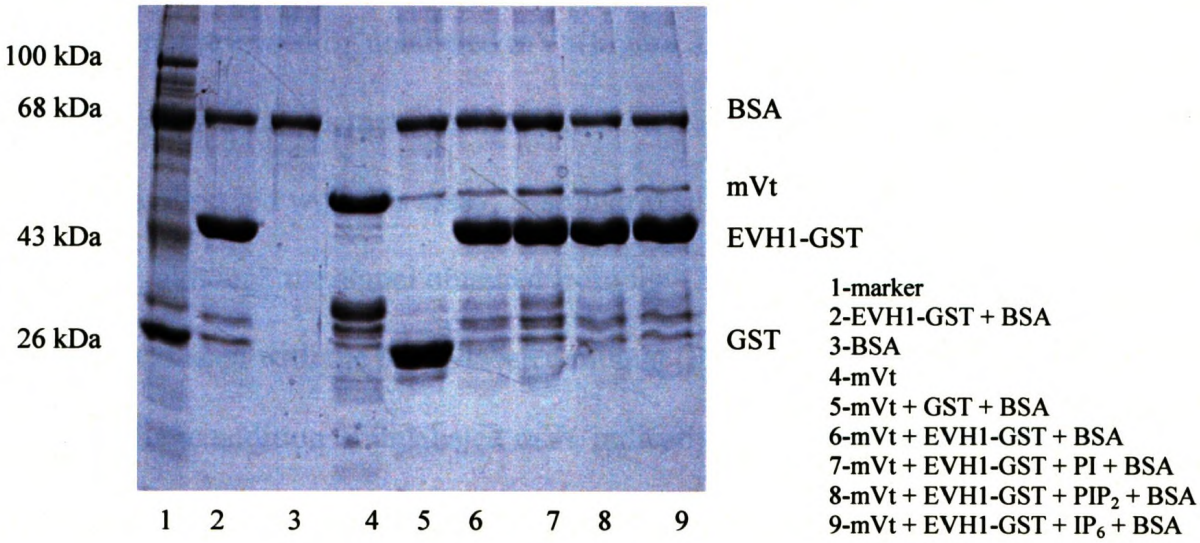

Figure 3.4: GST pull-down assay in the presence and absence of lipids. A. Pull-down with mVt and mVt (877). All samples are precipitates with the exception of lanes 3 and 6, which are representative of total protein in assay. B. Pull-down with mVt and lipids. Lipids used were PI, and PIP_2. All samples are precipitates with the exception of lane 4, which is representative of total mVt in assay. Gel is stained with Coomassie stain.

supernatants were run on SDS-PAGE. The fluorescence in the supernatants was then assayed. A small, though not significant, decrease was observed with the mVt-FITC + EVH1-GST sample (Figure 3.5). However, GST alone led to a larger decrease. Thus, no binding was apparent. This result was seen with three separate experiments.

Another sensitive assay that was also tested involved fluorescence perturbation. This is an efficient assay, as it measures binding in solution without the need to separate any of the components at any point. Both of the mVt mutant constructs were labeled with either CPM or NPM for this assay, with the idea that the aromatic nature of these fluorophores might substitute for phenylalanine. There was indeed an increase in fluorescence seen after the addition of EVH1-GST to the NPM-labeled mVt, but this increase was not reversed by unlabeled mVt (Figure 3.6A). When the fluorescence due to EVH1-GST on its own was measured, a similar increase was seen. Thus only background changes were observed with this assay. A similar result was seen with the CPM-labeled site 1 mutant, although the signal obtained from the CPM-labeled mutant was much higher than was seen with the NPM-labeled mutant (Figure 3.6B). Again, no decrease was seen with the addition of unlabeled mVt, indicative of an increase due solely to background.

As both VASP and metavinculin interact with actin, an actin binding assay was utilized to see if the actin binding had any effect on the interaction of the mVt and the EVH1 domain. In this assay, the actin forms long polymers that are easily pelleted, allowing an interaction with actin to be detected simply by the presence of the ligand in the pellet. The EVH1 domain was not pulled down with the actin by itself, or with the actin-mVt complex (results not shown), again suggesting little interaction.

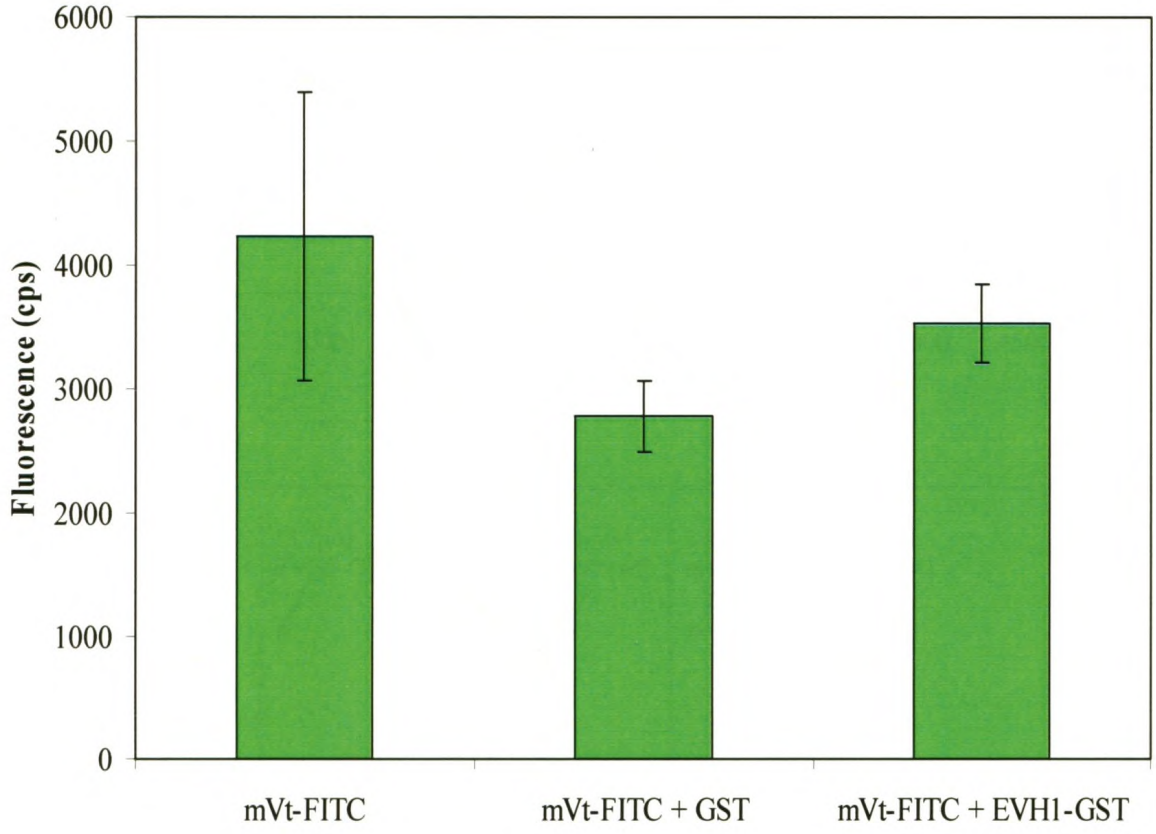

Figure 3.5: Fluorescence supernatant depletion assay. Fluorescence remaining in supernatant was measured after glutathione bead pull-down. n=3, p=0.10. Error bars represent standard deviation. Student's t-test employed.

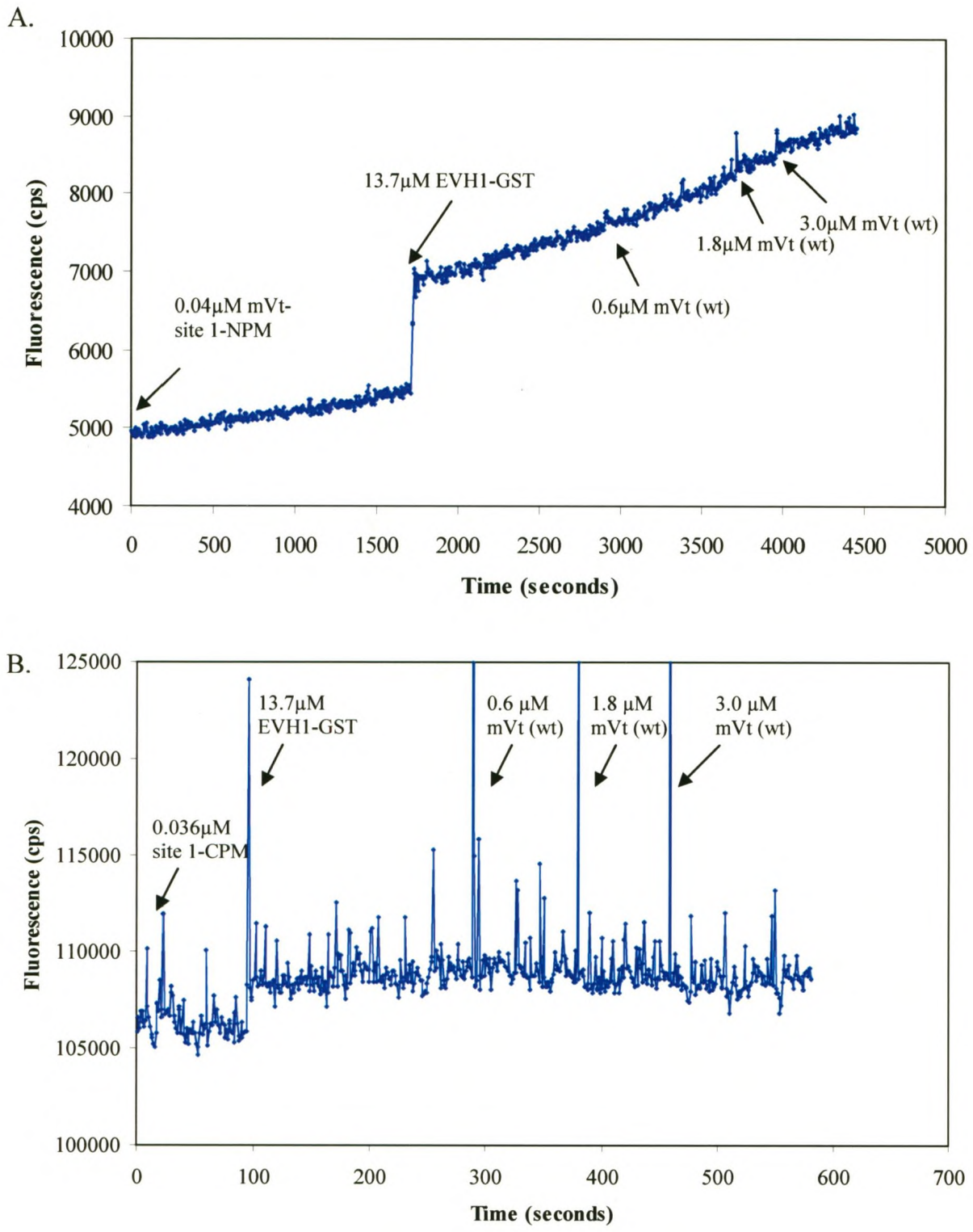

Figure 3.6: Fluorescence perturbation assay with mVt-site 1-NPM and mVt-site 1-CPM. A. NPM was excited at 338nm and emission was measured at 375nm. B. CPM was excited at 384nm and emission was measured at 469nm. n=3.

After various *in vitro* attempts failed to detect any binding, even though site 1 was intact, I wondered whether a vital factor(s) for the binding to occur were missing, and an *in vivo* assay was needed. To approach this, mVt-pEGFP, which expresses the construct with a GFP tag, and VASP-pcDNA3.1 (+), which expresses an untagged construct, were transfected into a human osteosarcoma epithelial cell line (U2OS). After harvesting the cells, the lysates were immunoprecipitated with anti-GFP antibody, and anti-VASP was used in a western blot. VASP was readily detected in lysates, but not in the precipitates (Figure 3.7A, lanes 4 to 6), at a molecular weight of approximately 43kDa. The VASP antibody labeled a band in the untransfected lysate sample, (Figure 3.7A, lane 6), which based on its size is likely endogenous VASP. When tested with VASP expressed in *E.coli*, the antibody did react, implying the antibody was in fact labeling the correct target. No increase in VASP is visible between the untransfected and transfected samples, most likely because of the large amount of endogenous VASP that is present. To confirm that the immunoprecipitation had indeed worked, the blot was reprobed with anti-GFP. The GFP-labeled mVt, as well as the GFP control, were readily detectable in the precipitates, as well as in the lysates, albeit at a lower intensity (Figure 3.7B, lanes 1 and 4). The bands previously identified with the VASP antibody are still visible after probing with anti-GFP.

At this point, I decided to test the assay that had been used by other groups studying VASP and vinculin, despite its disadvantages. In this assay, one binding partner is immobilized by binding to nitrocellulose and probed with the other binding partner, followed by an antibody detection system. The main disadvantage with this type of assay is that very little is known about what is happening to the protein when it is immobilized on the nitrocellulose membrane. Proteins irreversibly stick to the membrane but may

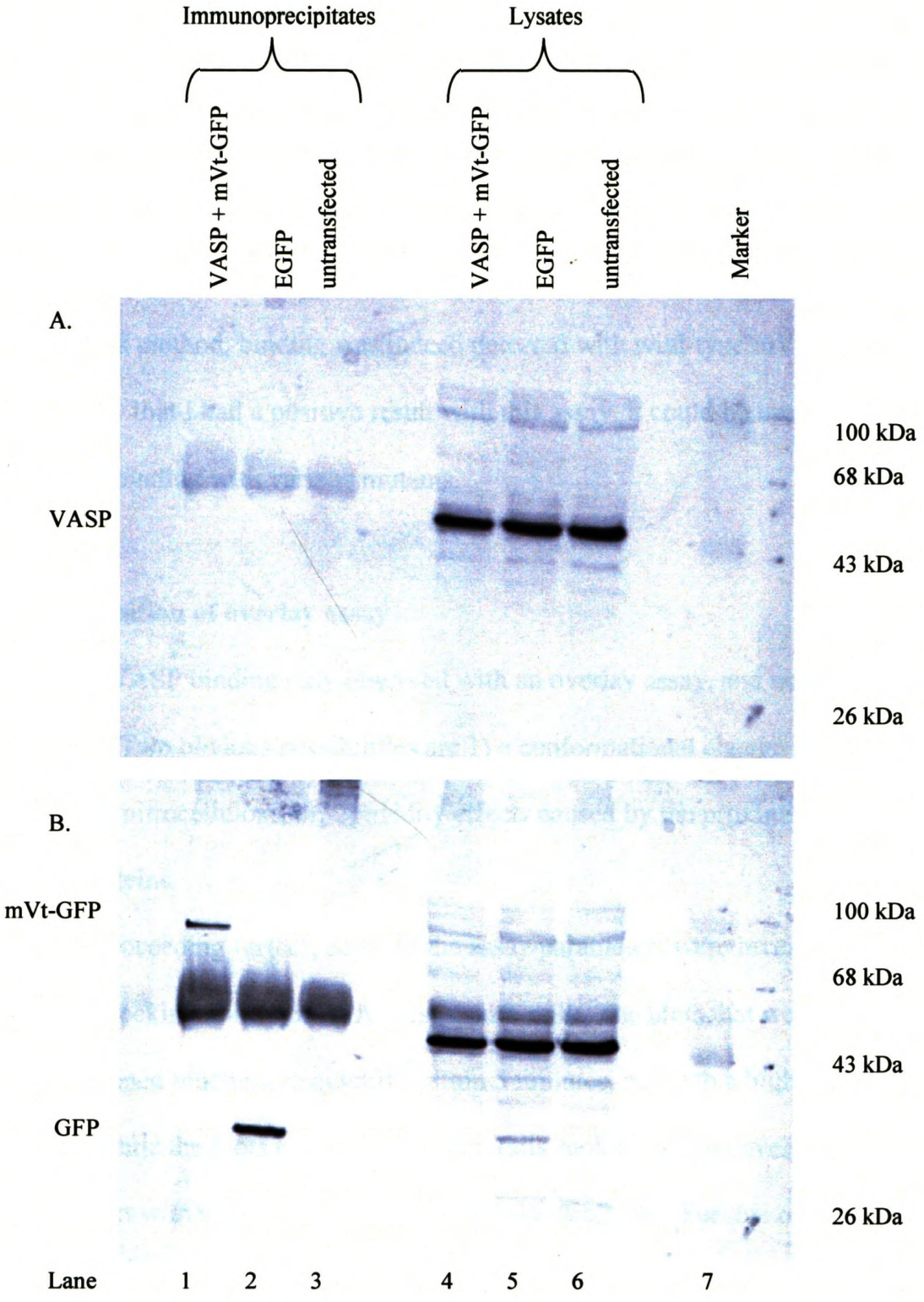

Figure 3.7: Western blots of immunoprecipitates from lysates of U2OS cells. A. Blot of anti-GFP immunoprecipitates with monoclonal anti-VASP, developed with alkaline phosphatase reagents. B. After membrane was blocked, it was probed with anti-GFP.

change conformation. We know this is true in some cases, as blotted vinculin binds F-actin, in contrast to soluble vinculin (Ruhnau and Wegner 1988; Johnson and Craig 1995). Another disadvantage is in the non-ideal kinetics of the assay, making it difficult to quantify the results (see below). However, the assay proved to be useful in identifying the interaction.

Using this method, binding was indeed detected with wild-type mVt (Figure 3.8, dots 3 to 5). Now that I had a positive result with this assay, it could be used to characterize the binding with various mutants.

3.4. Characterization of overlay assay

Why is VASP binding only observed with an overlay assay, and not in any of the solution assays? Two obvious possibilities are 1) a conformational change is induced by blotting onto the nitrocellulose, or, 2) avidity effects caused by the proximity of immobilized proteins.

Before proceeding further, some of the assay parameters were investigated, one of which was the blocking ability of BSA versus skim milk. The blots that were blocked with BSA developed much more quickly, within 5 minutes, but with a higher background (Figure 3.9A), while the blots blocked with skim milk took longer to develop, taking up to 15 minutes, but with a much lower background (Figure 3.9B). For this reason, skim milk was employed in all further blots. In other experiments, it was found that spots were more intense with a longer incubation with the monoclonal anti-GST antibody, so all blots were left overnight, from 14 to 17 hours, with this probe.

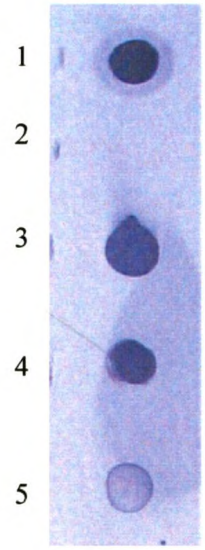

Figure 3.8: Nitrocellulose overlay assay. Wild-type mVt was dotted onto blots, EVH1-GST was allowed to bind and an antibody detection system was used to detect GST. Buffers contained 3% BSA for blocking.

A.

1-GST – 1µg
2-BSA – 1µg
3-Vt877 – 1µg
4-mVt – 1µg
5-mVt – 100ng
6-mVt – 10ng

B.

1-BSA – 1µg
2-GST – 20ng
3-mVt – 1µg
4-mVt – 500ng
5-mVt – 100ng

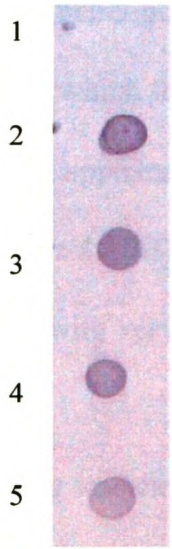

Figure 3.9: Nitrocellulose overlay assay with wild-type mVt blocked with BSA or skim milk. A. Blocking with 3%BSA, 5 minute development. B. Blocking with 5% skim milk, 15 minute development.

To make the assay as accurate and quantitative as possible, its linearity was investigated. Spot intensity was measured with the AlphaEase imaging software using an AlphaImager, (Alpha Innotech), which produces an integrated density value (IDV) defined as the sum of all of the pixel values within a chosen area, with white equal to 0 and black equal to 255. A representative background area for each blot was chosen and subtracted from the IDV value for each dot.

As a first step GST alone was dotted on nitrocellulose. Linearity with time and protein concentration was tested, with ranges from 2.5 to 15 minutes, and 10ng to 100ng of protein (Figure 3.10, A and B, respectively). The higher concentrations of GST appear to reach near saturation within the first 5 minutes, after which the increase is minimal (Figure 3.10A). With regard to protein concentration, it appears that the linear range does not continue past an IDV of between 60 and 100 (Figure 3.10B). It appears that a true linear range could be achieved, but at very short times with very low protein concentrations.

Next, the linear range of the mVt-EVH1 binding was examined. Again, a range of development times and protein concentrations were used. The development times were the same as with the GST alone, from 2.5 to 15 minutes, while the mVt protein amounts used varied from 100ng to 1μg (Figure 3.11, A and B, respectively). Unlike the linearity with time of the GST on its own, the entire assay appears to have a longer linear range, up to 10 minutes (Figure 3.11A). However, with a development time of 15 minutes, as the amount of mVt is increased a roughly hyperbolic curve is produced (Figure 3.11B). In the range of 100ng to 1 μg this could be approximated by a straight line ($R^2 = 0.77 - 0.97$), but only at a development time of 15 minutes.

A.

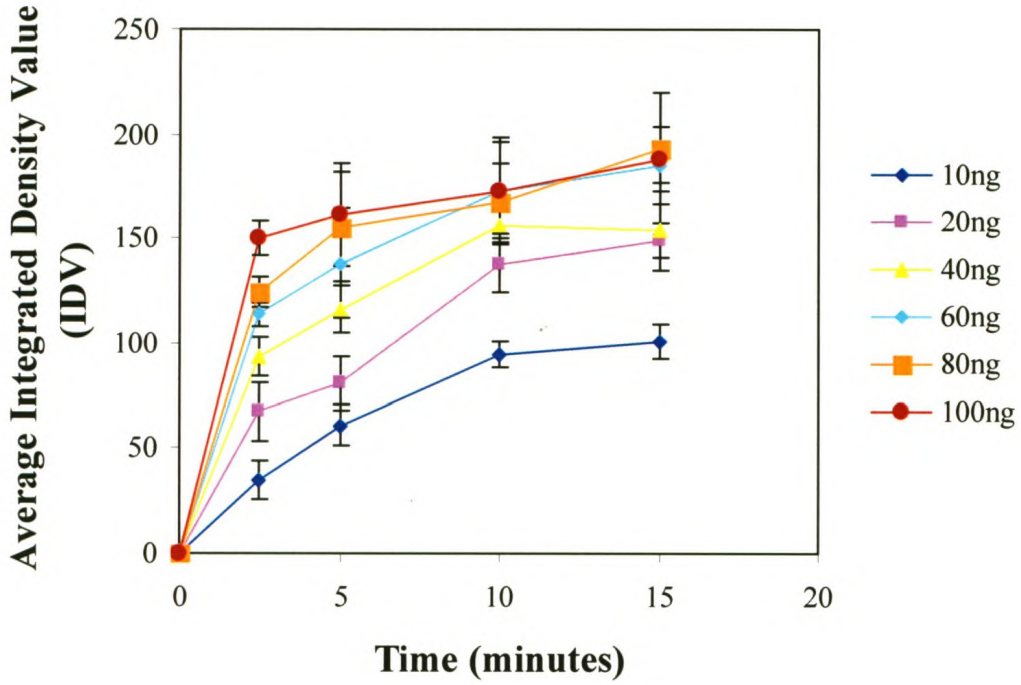

B.

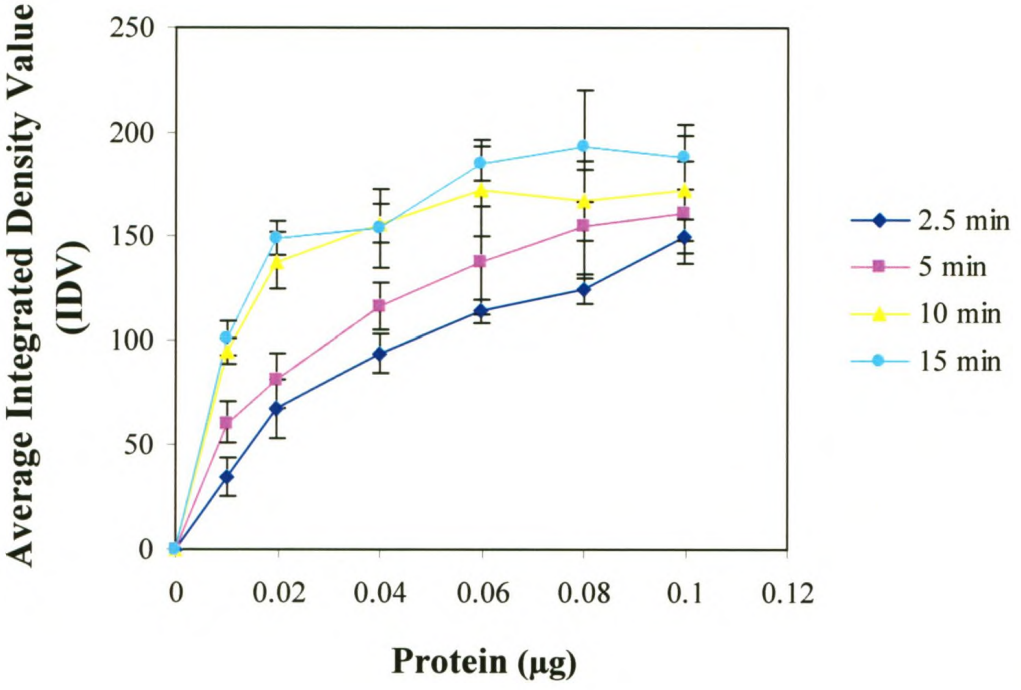

Figure 3.10: GST detection. GST alone was dotted onto the membrane, and an antibody detection system was used. A. Average IDV versus time, from 2.5 to 15 minutes. B. Average IDV versus protein concentration, from 10ng to 100ng. *n*=3, Error bars represent standard deviation.

A.

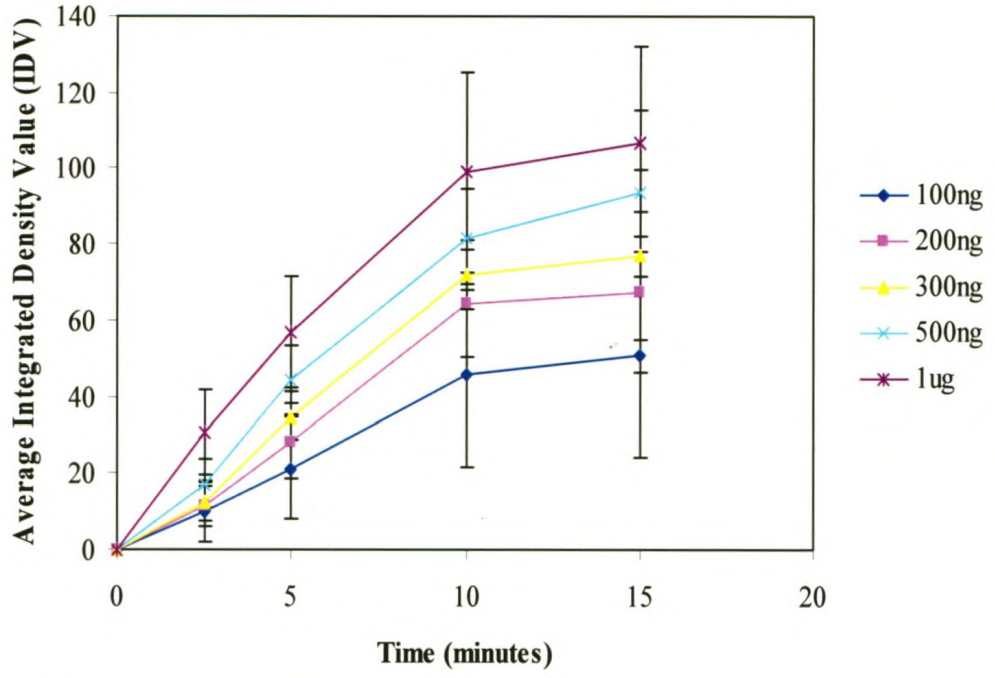

B.

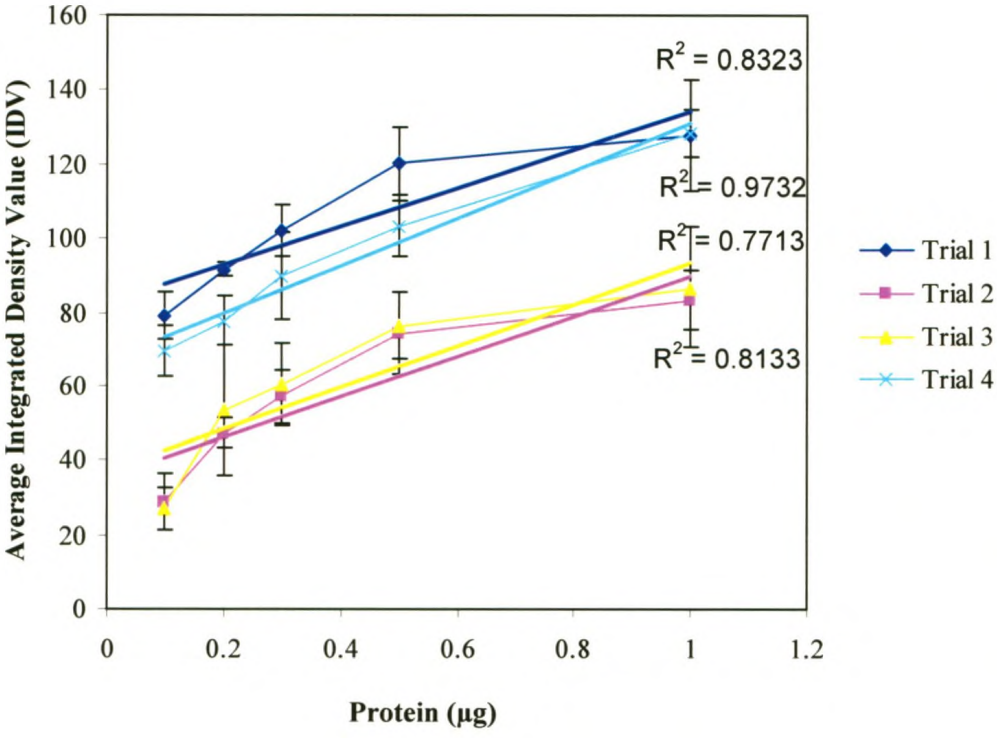

Figure 3.11: mVt detection. mVt was dotted onto the membrane, followed by binding with EVH1-GST, and a subsequent antibody detection system. A. Average IDV versus development time, from 2.5 to 15 minutes. B. Average IDV versus mVt protein concentration, from 100ng to 1µg, after 15 minute development. *n*=4, Error bars represent standard deviation.

From these linearity experiments, standard assay conditions were adopted: every strip included 100ng, 500ng and 1μg dots of wild-type mVt and was developed for 15 minutes. This development time was taken for a number of reasons; the kinetics appear to be irregular, as the development past 10 minutes should continue to increase, at least at the lower protein concentrations, not plateau. This could be due to the precipitating substrate, creating access problems to the enzyme. Despite this, there is proportionality between the densities and various protein concentrations after 15 minutes. A shorter development time could have been used, but sensitivity problems would have been encountered, because of the low intensities. Within restricted concentrations (100ng to 1μg) a linear response was observed (Figure 3.11B). The signal arising from different amounts of mutant protein, as well as various other constructs investigated, was compared to that from the wild-type within this range.

In an effort to determine if a conformational change in metavinculin was causing the binding to be detected, the protein was first denatured and then transferred to the nitrocellulose membrane with the remainder of the assay performed exactly as the strips were done. GST alone and varying concentrations of the wild-type mVt were first loaded onto a 12% SDS-PAGE gel, which was then electrophoretically transferred to a nitrocellulose membrane. After completing the EVH1-GST binding and antibody detection, the binding was detected, albeit at a lower intensity then has been seen on the strips (data not shown). This implies that denaturing the protein had little effect on the interaction.

It is a possibility that the overlay assay detected the interaction because of the avidity effects created by dotting large quantities of the protein onto the membrane in a

small area. As one test of the idea that avidity effects are crucial, an identical amount of protein was dotted onto the nitrocellulose in various volumes. Dilutions were made up of both wild-type mVt, as well as a biotinylated-site 2 mutant complexed with avidin. As one avidin can interact with four biotin molecules, this complex should consist of four mVt molecules in close proximity. These dilutions ranged from volumes of 3µl to 1.2µL, in the hopes of seeing an increase in IDV with the lower volumes due to closer spaced molecules. With the wild-type mVt, despite an increase seen initially between 3µL and 2.5µL, the remaining dilutions show a progressive decrease in integrated intensity (Figure 3.12, A and B). The mVt-biotinylated-avidin complex showed a continuous decrease in intensity, the opposite of expected.

3.5. Characterization of interaction using overlay assay

The standardized overlay assay was used to compare the binding of wild-type mVt with various mutant proteins to examine the specificity of the interaction. The first comparison made was with the two site mutants. The site 2 mutant, which has only the known, F842 site, showed variable binding in different experiments, ranging from almost identical binding to noticeably decreased over the wild-type, with an average percentage of the wild-type of 65% ± 34 (Figure 3.13A). The site 1 mutant, which would only have the second putative site at F939 showed an almost undetectable amount of binding (Figure 3.13B), although a small amount of binding was detectable when BSA was used as a blocker instead of skim milk. Thus site 1 is clearly more important than site 2, but the latter did have some influence.

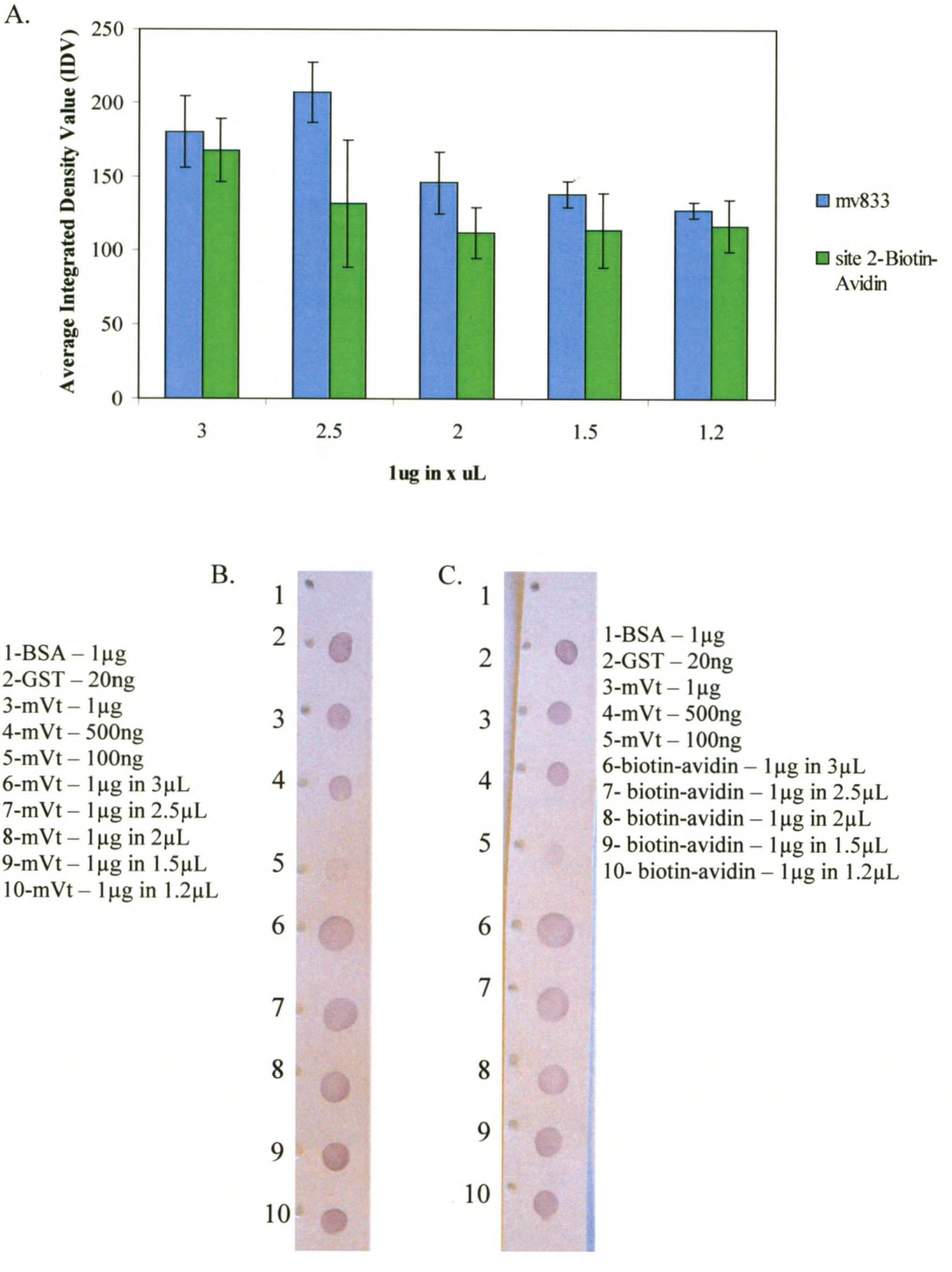

Figure 3.12: Avidity test of mVt and mVt-biotin-avidin complex. A. Graph comparing average IDV of mVt and mVt-biotin-avidin complex dilutions. B. mVt dilutions. C. mVt-biotin-avidin complex. *n*=3, Error bars represent standard deviation.

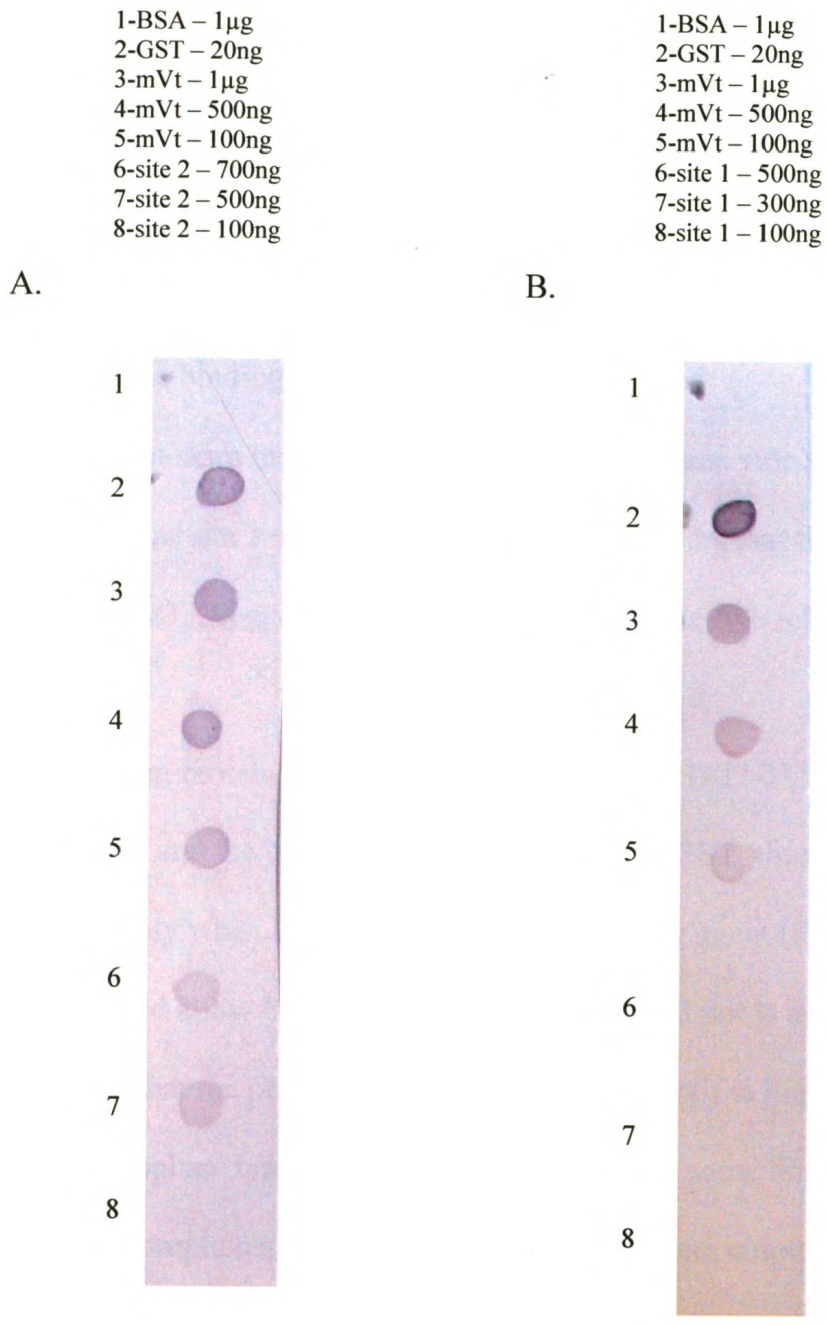

Figure 3.13: Nitrocellulose overlay assay with site 1 and site 2 mutants. A. Blot of wild-type mVt and site 2 mutant. B. Blot of wild-type mVt and site 1 mutant. n=4.

Another important comparison that was made to the wild-type mVt was the Vt833, which only contains site 1. As expected, binding was detectable with Vt833, but at a slightly lower intensity than wild-type mVt (Figure 3.14A). Binding of mVt was also compared with the full-length vinculin molecule, which again contains only site 1, and there was no binding detected with the full-length vinculin (data not shown). The Vh construct, which contains site 1, was also compared to mVt, and no binding was seen with the Vh (data not shown). A smaller portion of the Vh, referred to as domain 3, also contains site 1. This construct showed detectable binding, but only when BSA was used as a blocking agent, and not skim milk (data not shown). All of these vinculin constructs would be expected to bind as site 1 should be exposed, but it appears that the only construct binding is the Vt833, suggesting a need for more than the five residues in the binding motif.

When the interacting proteins were reversed, with the EVH1 (1-115)-his being dotted onto the membrane, and the binding performed with mVt-GST, there was an interaction detected, but only when BSA was used as the blocking agent (Figure 3.14B). The reason why BSA would allow binding while skim milk would not is unknown.

It has been shown that the phenylalanine in the binding motif is important, but it can be replaced with tryptophan, tyrosine or lysine and still retain some binding (Ball, et al. 2000). A number of fluorophores that are aromatic in nature were employed to determine if binding could be restored with both of the sites, or if the requirements for these sites were somehow different. The labeled mutants were compared to the wild-type mVt, as well as to the unlabelled mutant. When mVt833 site 2 labeled with CPM was dotted, binding was increased relative to the unlabeled mutant, and intensity comparable

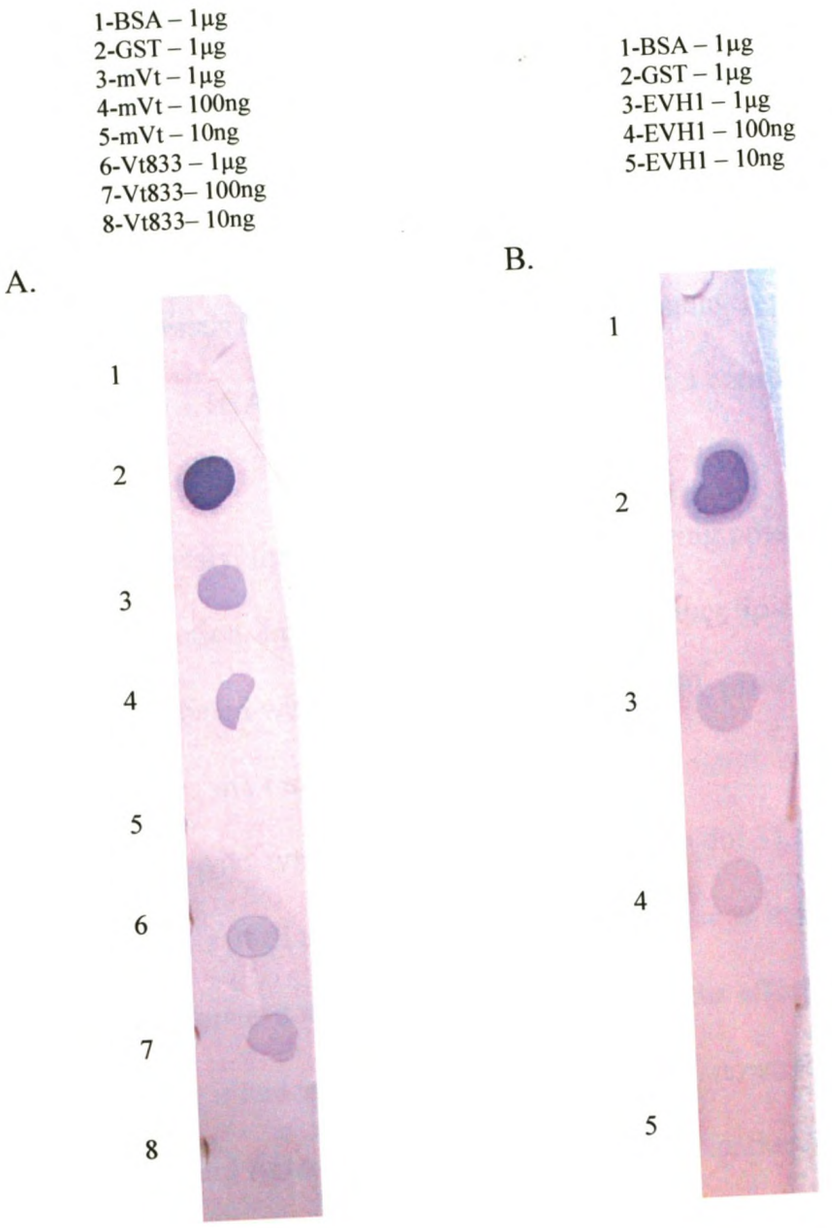

Figure 3.14: Nitrocellulose overlay assay with Vt833 and EVH1. A. Blot of wild-type mVt and Vt833. B. Blot of EVH1-his, binding done with mVt-GST.

to mVt was seen (Figure 3.15A and B, dot 9 – 11). Likewise, CPM-labeled site 1 also showed an increase in binding, although nowhere near the intensity of mVt (Figure 3.15A and C, dot 9 – 11).

Site 1 labeled with NPM and DTNB were also tested to see whether other compounds could restore binding. Interestingly, both of these were also able to restore binding to the EVH1-GST. The NPM-labeled construct had binding less than that of the wild-type, but there was a definite increase over the non-labeled site 1 mutant (Figure 3.16A and D, dots 8 and 9 versus 6 and 7). The DTNB-labeled mutant was also effective in restoring binding, (Figure 3.16 A and E, dots 9 and 10), but is not comparable to wild-type intensity.

As mentioned previously, lipids have been identified as being possible enhancers of the VASP-vinculin interaction. In an attempt to determine whether lipids have this ability or not, mVt was incubated with varying concentrations of PI, prior to dotting onto the nitrocellulose membrane. mVt incubated with an equimolar amount of PI showed no change in intensity from the wild-type (Figure 3.17B, dot 6 versus dot 3), while the mVt with 20 and 100-fold amounts of PI also showed no significant change in intensity (Figure 3.17B, dot 7 and 8 versus dot 3). I also wanted to look at the effect of NaCl concentration on the binding interaction on nitrocellulose, as it is known that the interaction between EVH1 and ActA peptide is mainly hydrophobic, due to proline pyrrolidine rings packing into the hydrophobic grooves between the closely spaced aromatic side chains of the aromatic triad in EVH1 (Zimmermann, et al. 2003). The NaCl concentration under standard conditions was 140mM, and the concentrations tested were 5mM, 50mM, 200mM, and 500mM NaCl. The wild-type mVt, the two binding site mutants, as well as Vt833 were used to determine whether varying NaCl concentrations

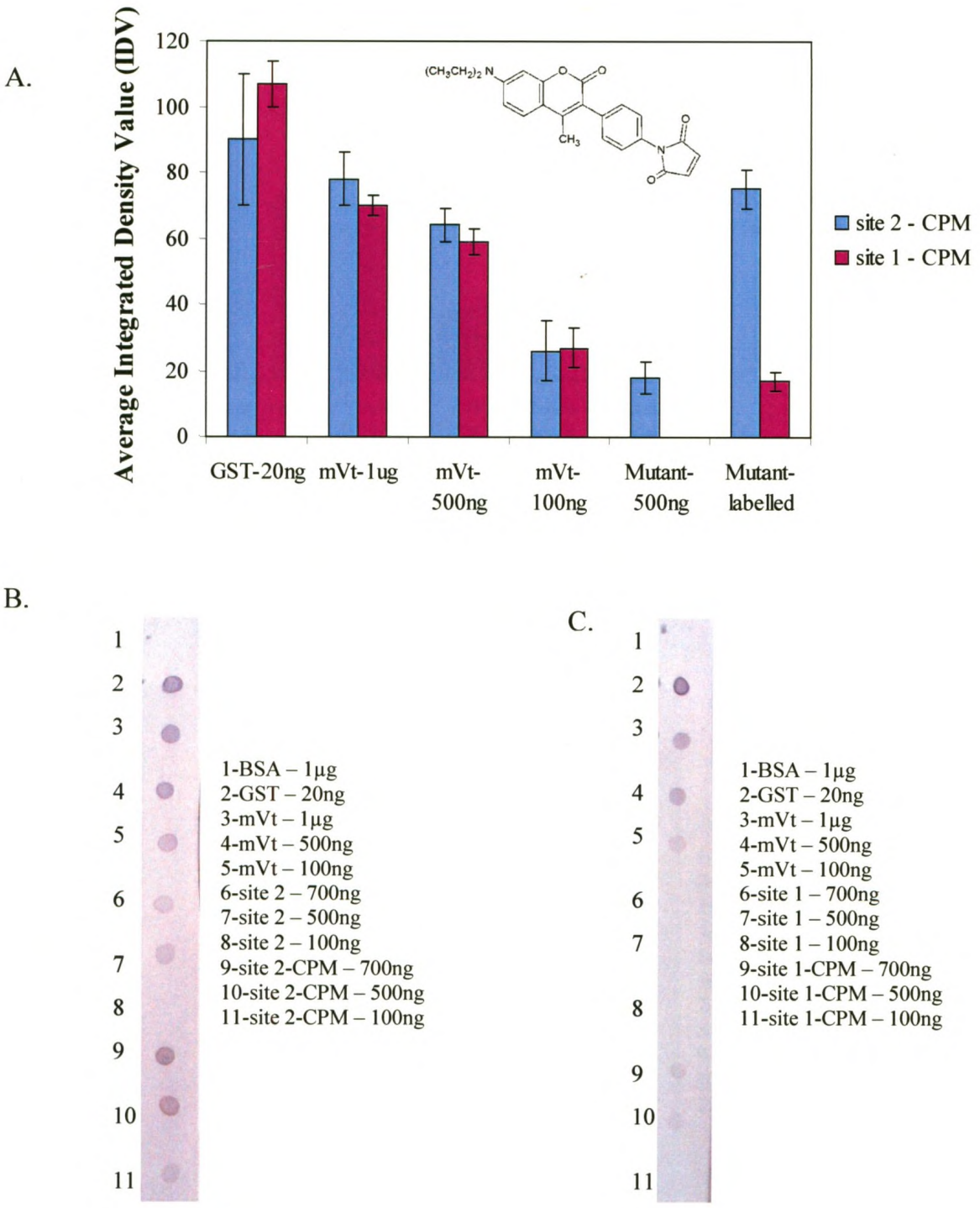

Figure 3.15: Nitrocellulose overlay assay with CPM-labelled mutants. A. Graph of binding intensities with and without CPM labelling. Inset-Structure of CPM. B. Blot comparing site 2 and site 2-CPM. C. Blot comparing site 1 and site 1-CPM. *n*=6, Error bars represent standard deviation.

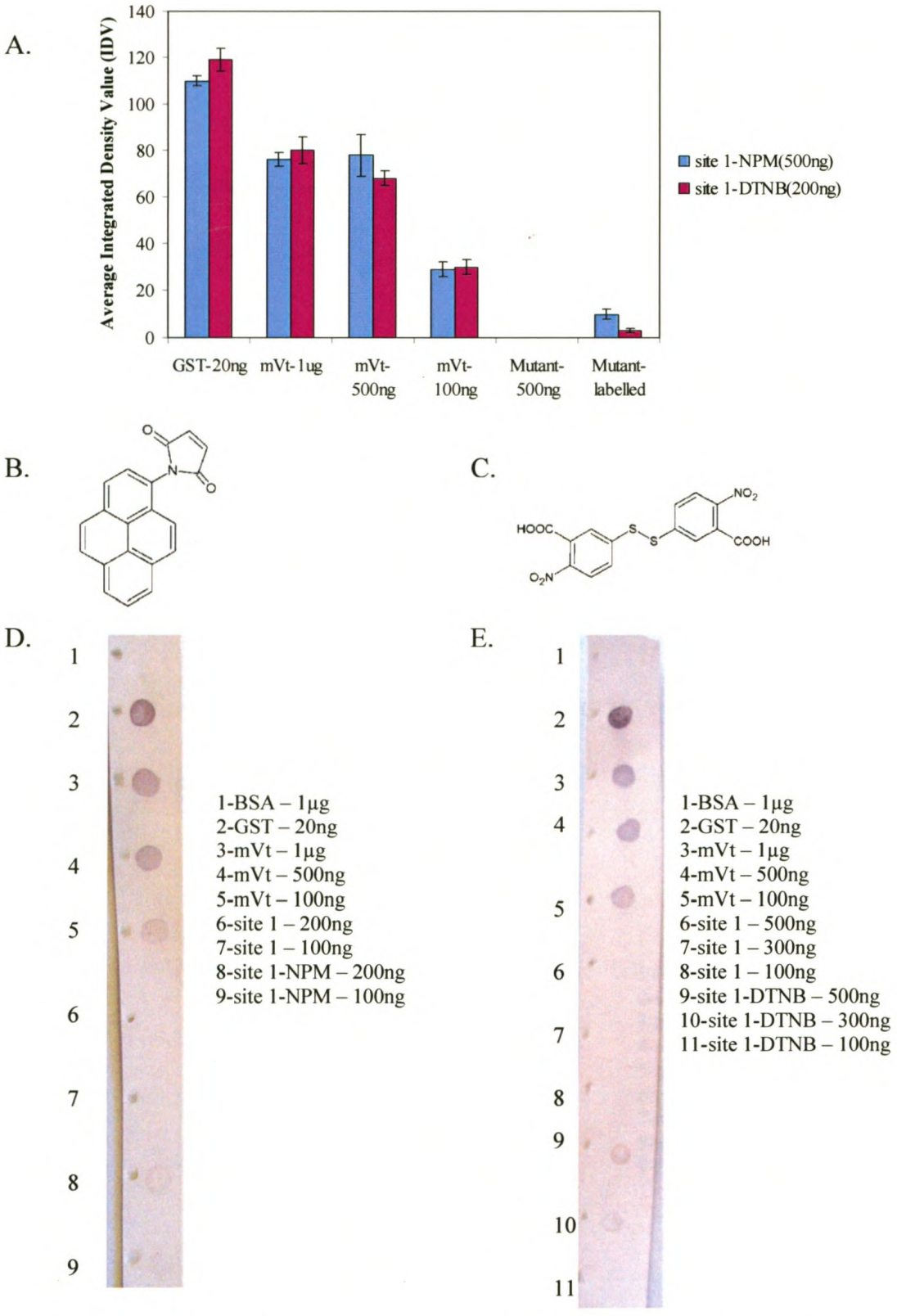

Figure 3.16: Nitrocellulose overlay assay with NPM and DTNB-labelled site 1 mutants. A.Graph of binding intensity with and without labelling. B. Structure of NPM. C. Structure of DTNB. D. Blot comparing site 1 and site1-NPM. E. Blot comparing site 1 and site 1-DTNB. n=4, Error bars represent standard deviation.

A.

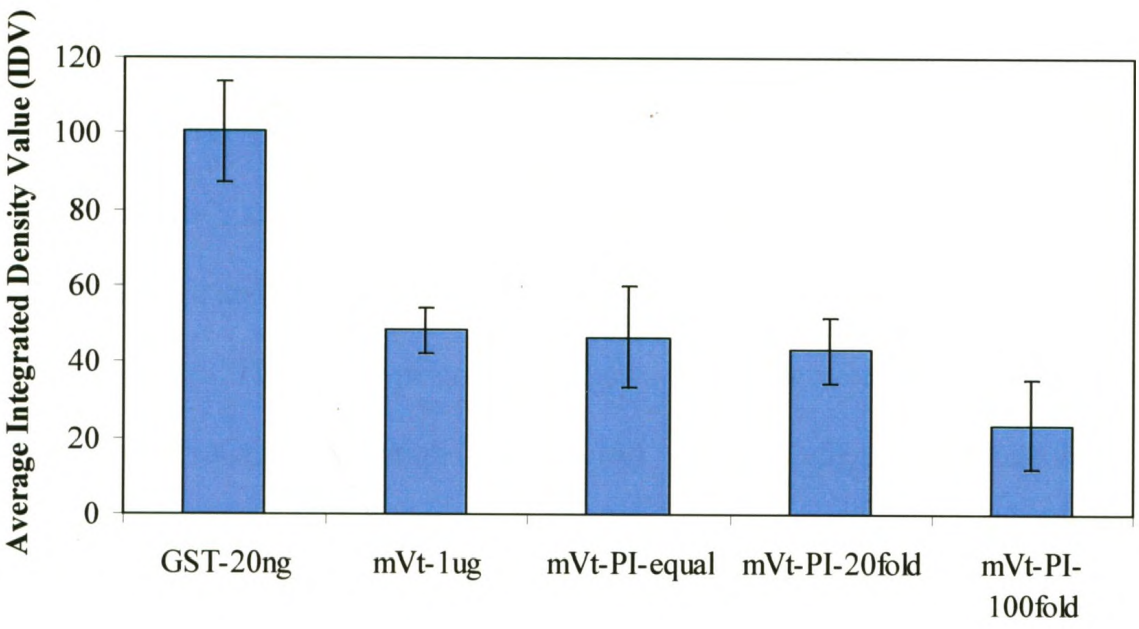

B.

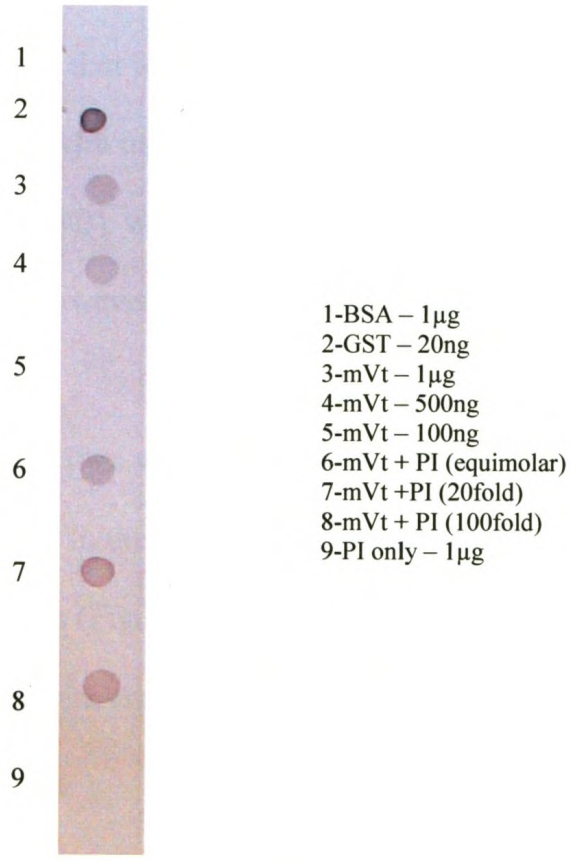

Figure 3.17: Nitrocellulose overlay assay with lipids. A. Graph of binding intensity of varying samples with and without PI. B. Blot of proteins dotted with or without PI. *n*=6, Error bars represent standard deviation.

affected the interaction. At the low range of 5mM, binding was detectable with all of the mutants, even the site 1 mutant (Figure 3.18A), while a concentration of 50mM appeared to decrease the binding from that seen with 5mM, with the site 1 and Vt833 constructs being greatly reduced (Figure 3.18B, dots 9-14). As the NaCl concentration increased from 140mM to 200 and 500mM, binding was again reduced from that seen with 5mM NaCl (Figure 3.18C, D and E). The binding through the site 1 mutant and Vt833 is lost with 140mM NaCl and up, while the site 2 mutant appears to be least affected by the NaCl concentration. The wild-type construct shows a slight decrease in binding over the higher ranges of NaCl concentration (Figure 3.18A – E, dots 3-5), more so than the decrease seen with site 2 mutant (Figure 3.18A – E, dots 6-8).

The effect of pH on the nitrocellulose binding interaction was also investigated with the goal of elucidating more about the interaction taking place. The standard pH of the assay was 7.5, and the other pH values that were tested were 6.0, 8.0 and 9.5. Out of the three, pH 8.0 appeared to be optimal, with the highest intensity binding occurring with regards to all of the constructs (Figure 3.19B), while pH 6.0 and 9.5 blots had slightly lower intensities (Figure 3.19A and B). However, the differences were not statistically significant.

The possible involvement of metal ions was examined through the addition of EDTA to the blocking and binding buffers in the binding assay. Interestingly, a decrease in binding was seen with all of the proteins (Figure 3.20A and B), while the decrease is restored through the addition of an equimolar amount of Ca^{2+} (Figure 3.20A and C).

1-BSA – 1µg
2-GST – 20ng
3-mVt – 1µg
4-mVt – 500ng
5-mVt – 100ng
6-site 2 – 1µg
7-site 2 – 500ng
8-site 2 – 100ng
9-site 1 – 1µg
10-site 1 – 500ng
11-site 1 – 100ng
12-Vt833 – 600ng
13-Vt833 – 300ng
14-Vt833 – 60ng

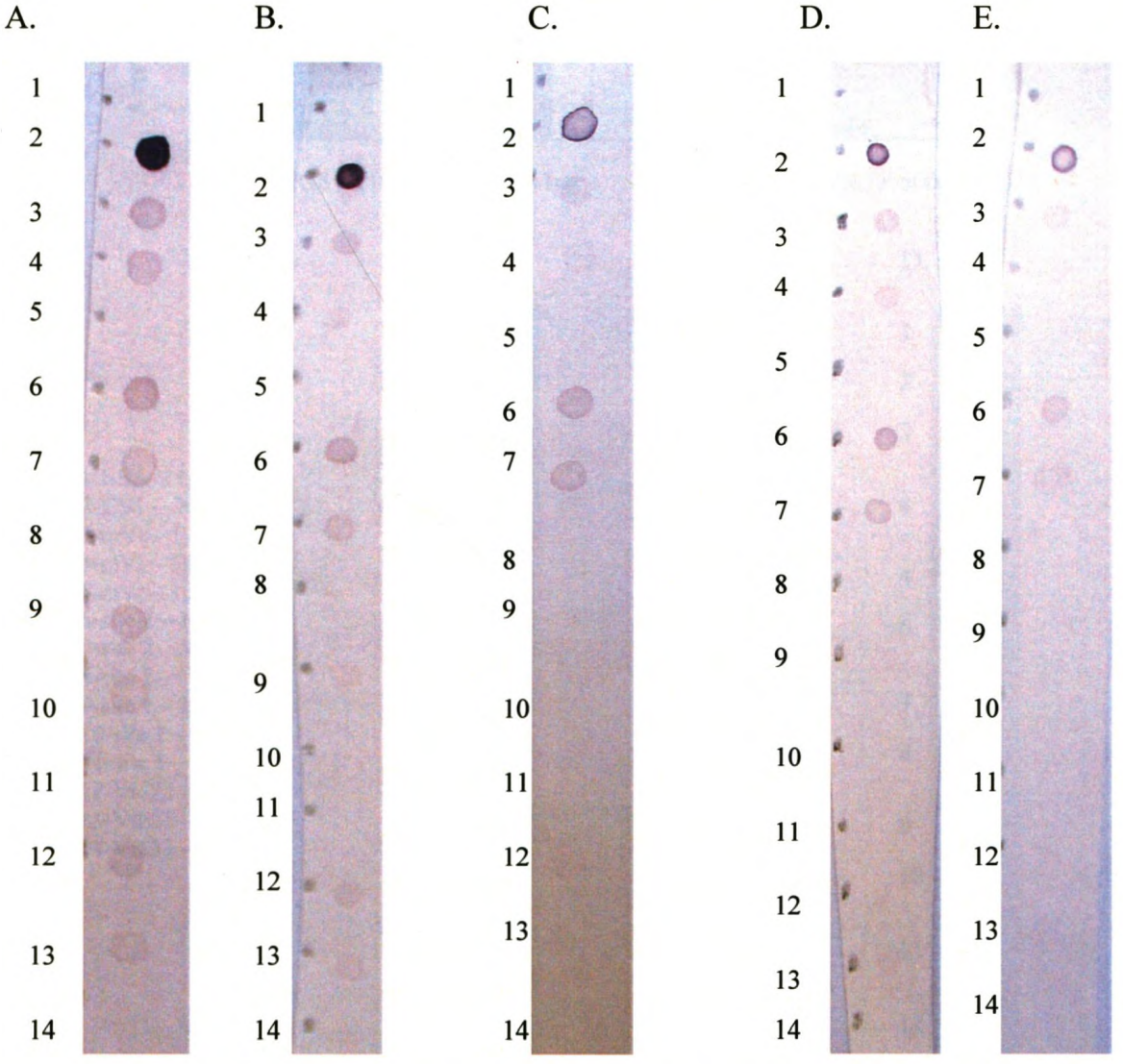

Figure 3.18: NaCl effects on nitrocellulose overlay assay. A range of salt concentrations were employed, from 5mM to 500mM. A. Blot using 5mM NaCl. B. Blot using 50mM NaCl. C. Blot using 140mM NaCl. D. Blot using 200mM NaCl. E. Blot using 500mM NaCl.

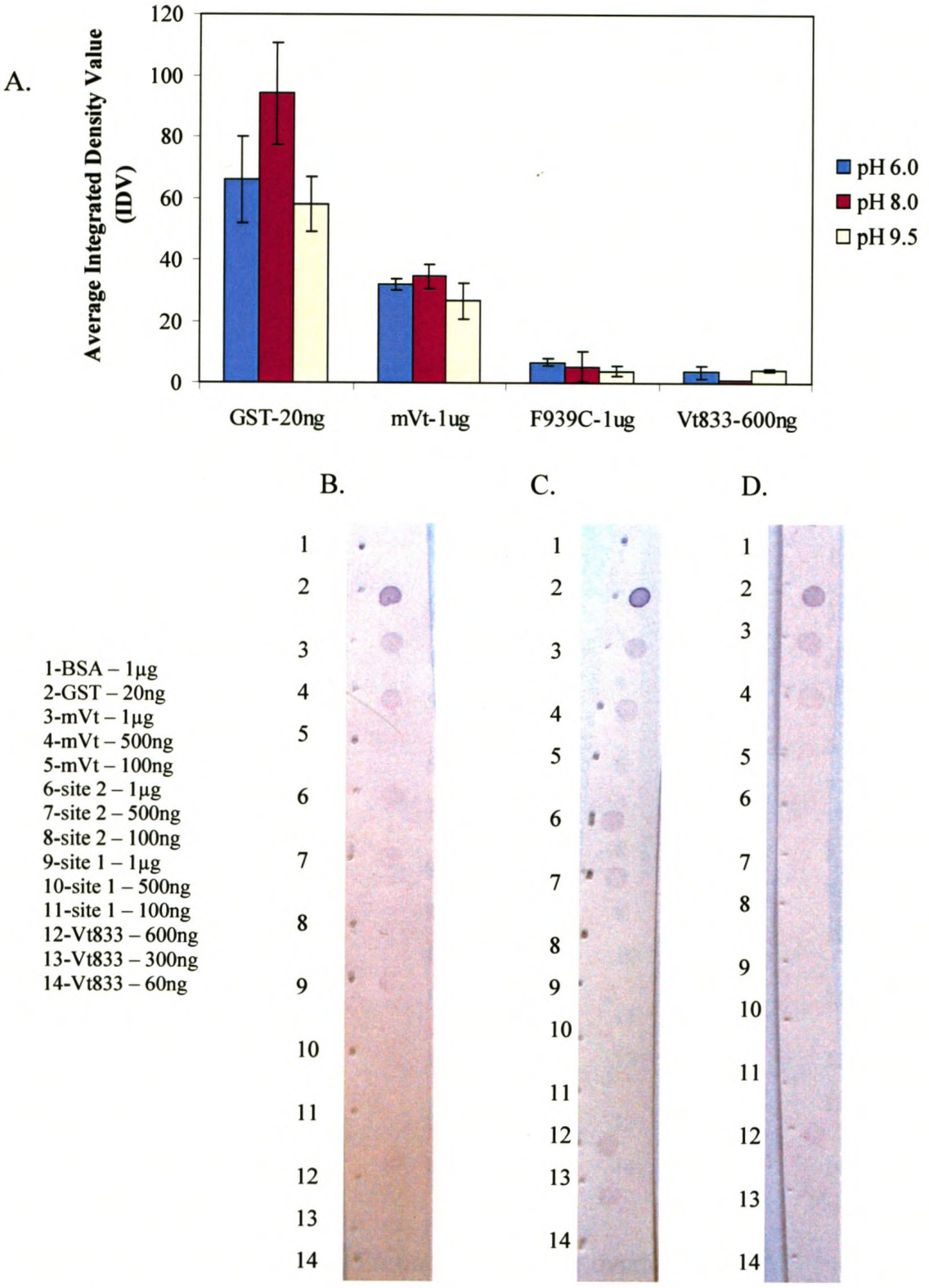

Figure 3.19: pH effects on nitrocellulose overlay assay. A. Graph of pH effects on binding. B. Blot with pH 6.0 buffer. C. Blot with pH 8.0 buffer. D. Blot with pH 9.5 buffer. *n*=3, Error bars represent standard deviation.

A.

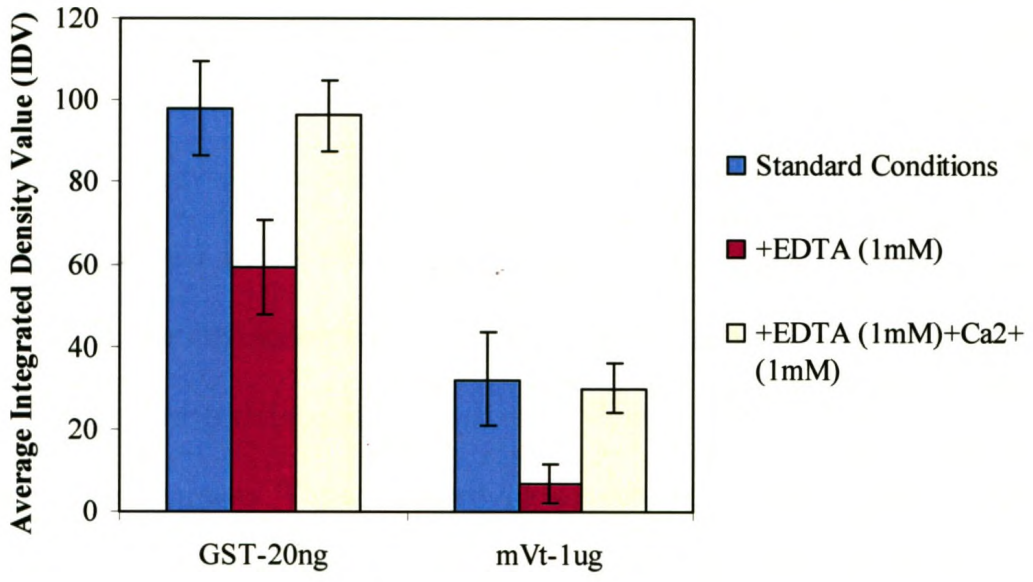

B. C. D.

1-BSA – 1µg
2-GST – 20ng
3-mVt – 1µg
4-mVt – 500ng
5-mVt – 100ng
6-site 2 – 1µg
7-site 2 – 500ng
8-site 2 – 100ng
9-site 1 – 1µg
10-site 1 – 500ng
11-site 1 – 100ng
12-Vt833 – 1µg
13-Vt833 – 500ng
14-Vt833 – 100ng

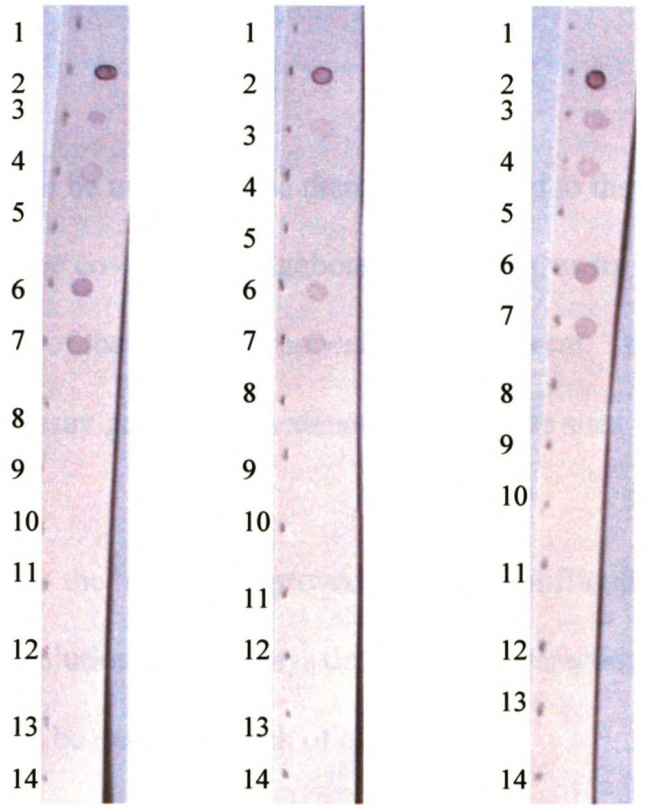

Figure 3.20: Effect of EDTA on nitrocellulose overlay assay. A. Graph comparing binding intensity with or without EDTA and Ca^{2+}. B. Blot without EDTA. C. Blot with 1mM EDTA. D. Blot with 1mM EDTA and 1mM Ca^{2+}. *n*=6, Error bars represent standard deviation.

CHAPTER 4

DISCUSSION

The intent of this study was to examine the interaction between VASP and metavinculin through a second, putative binding site identified in the metavinculin insert, as well as to characterize the interaction occurring through the known vinculin site. Site-directed mutagenesis of an essential residue in both of the binding sites to a cysteine was used to analyze the sites separately. The results provide evidence that the second site may indeed be a VASP binding site, but with a lower affinity than the known site, and also imply that the two sites may be mediated by different non-covalent forces.

4.1. Detecting the interaction

The prolines in the motif could be in a loop, and therefore exposed to the solvent. The phenylalanine, however, could be covered by neighbouring residues, as its hydrophobic nature would prefer the interior of the protein as opposed to the solvent. This does not seem to be the case, as the DTNB assay gave clear evidence that both the sites are exposed to the solvent.

The development of an assay to detect the interaction proved to be more difficult than expected. The reason why none of the solution phase assays detected the interaction is unknown, but a possible explanation could be due to the lack of efficient oligomerization of the two proteins, which could reduce the avidity of the interaction. Some other possible explanations as to why no interaction was detected with the solution phase assays could be a lack of a cofactor required for binding, incorrect conditions, or even the protein being in the wrong conformation for binding to occur. The interaction

does have a relatively low affinity, between 1 and 200μM (Ball, et al. 2000) according to assays with peptide, but the literature has shown a number of groups have been able to detect binding through solution phase assays (Brindle, et al. 1996; Huttelmaier, et al. 1998). However, the difference between what these groups did and what I did was that they were using the full-length VASP molecule, whereas I was using the EVH1 domain on its own, mainly due to problems with expressing the full-length protein in *E.coli*.

When these groups performed the above solution phase binding assay using truncated forms of the VASP protein, either lacking the N- or C-terminal, binding was lost (Brindle, et al. 1996; Huttelmaier, et al. 1998). The loss of binding seen without the C-terminal domain is likely due to the lack of oligomerization, as this domain is involved in the tetramerization of the protein (Gertler, et al. 1996; Zimmermann, et al. 2002). Multimerization would be expected to create an avidity affect; four EVH1 domains linked together could interact much more strongly with a multimeric ligand than a single EVH1 domain on its own (Machner, et al. 2001). The low affinity of the monomeric interaction is most likely why none of the solution assays I attempted showed detectable binding. GST is a dimeric protein (Wilce and Parker 1994), and fusions may mimic ligand-induced dimerization (Yan, et al.1995), and is able to partially reactivate a protein lacking its tetramerization domain *in vitro* and *in vivo* (Maru, et al. 1996). Avidity effects require both binding partners to be multimers, so GST tagging of EVH1 might not be enough.

As mentioned previously, we know that metavinculin also has the capability to oligomerize in some circumstances (Huttelmaier, et al. 1997). It is also notable that talin has many vinculin binding sites (Hemmings, et al. 1996), and could serve to create a vinculin multimer. Perhaps if another tag that is known to dimerize could be fused to the

metavinculin, the interaction would be detectable with the solution phase assays I employed.

The *in vivo* assay which I attempted was similar to that which another group had tried with vinculin and VASP (Huttelmaier, et al. 1998). In that case, binding between VASP and vinculin was detected, but required chemical cross-linking. I attempted this assay without the cross-linking with the intent of seeing whether the interaction could be detected using metavinculin, with its two possible binding sites. This was not the case, and one possible explanation for the apparent lack of binding is that the GFP tag may have interfered with the interaction, as site 1 is only 10 residues from the N-terminus, where the GFP was fused.

In the solid phase overlay assay multiple metavinculin molecules would be stuck in presumably close proximity on the membrane, mimicking the close proximity that metavinculin molecules could have in focal adhesions. This, coupled with the dimerized EVH1-GST domain, would be expected to give avidity effects. I attempted to test this idea by diluting metavinculin before dotting, to increase the spacing between molecules, but did not detect a decrease in binding (Figure 3.12). This does not mean that avidity is not involved, but this specific experiment may not have created the right conditions. A wider range of dilutions may be more revealing, but was not possible due to restrictions on protein detectability. A better way to test for avidity effects might be through the use of a linker to space the molecules set distances from one another on the membrane, if that were possible. To test for avidity effects in solution, it may be possible to link metavinculin molecules together before measuring binding.

An alternative possibility could be from a conformational change in metavinculin when dotted onto the blot, which could expose the second site in such a way that binding

was favourable, but would never exist *in vivo*. An example of this occurred with blotted vinculin that was probed with F-actin, and was shown to bind the probe, which does not occur with soluble vinculin (Ruhnau and Wegner 1988; Johnson and Craig 1995). As an indirect means of looking at whether a conformational change was involved, I tried blotting already denatured protein by using SDS-PAGE, followed by an electrophoretic transfer to the nitrocellulose membrane. The binding was detectable, albeit at a lower intensity (data not shown), indicating that denaturing the protein beforehand did not affect the binding; however, the protein may have renatured on the membrane. Although it is unknown what exactly is happening when a protein is transferred to nitrocellulose, it is thought that denatured proteins separated by SDS-PAGE are partially renatured once they are transferred to the membrane through the removal of SDS (Birk and Koepsell 1987; Klinz 1994). Once on the membrane, some proteins have been shown to be able to regenerate their enzymatic activity, or their ability to interact with ligands (Salehzada, et al. 1991; Strom, et al. 2006). In our case, it is possible that metavinculin is undergoing a conformation change once on the membrane that is resulting in an interaction with EVH1 that would not exist in solution, which could explain why there was no binding detected in the solution phase assays. However, this is difficult to test, while the avidity effects could be tested using a multimeric metavinculin. The theory of avidity effects is understandable, and may be the more likely of the two, but to determine this for certain, more experiments are required.

4.2. Characterizing the interaction

Once the overlay assay was standardized, I proceeded to analyze the interaction between metavinculin and EVH1 more closely. First and foremost, the site 1 mutant

showed no binding, with a few exceptions where only tiny amounts of binding where detected (Figure 3.13B). This indicated that site 2 alone is not a high affinity site. In the site 2 mutant results were somewhat variable, from equal binding to visibly reduced binding compared to wild-type (Figure 3.13A). The average binding seen with this mutant was 65% ±34 of the wild-type binding over 7 experiments. This implies that site 2 has an influence on the interaction with EVH1. The difference between the sites could be due to conformation or sequence, with site 2 having a much lower affinity then site 1.

As part of characterizing the interaction, different salt concentrations were tested. As mentioned previously, two types of non-covalent interactions are thought to occur between vinculin and the EVH1 domain: hydrophobic, and ionic. Increasing salt concentration has a negative effect on any ionic interactions (Horton, et al. 2002), but a positive effect on hydrophobic interactions between non-polar residues. Interestingly, at the low NaCl concentration binding appears to be of comparable intensities with all of the constructs, including the site 1 mutant (Figure 3.18A). As the salt concentration increased, the binding appeared to decrease most notably with the site 1 mutant and Vt833, while the wild-type and site 2 mutant showed smaller decreases in binding (Figure 3.18B-D). This result implies some differences in the interactions occurring between the two sites.

As mentioned previously, the interaction occurring between the EVH1 domain and its proline rich ligand is thought to be mediated through both ionic and hydrophobic forces via the flanking residues of the binding motif, mainly the residue immediately preceding the phenylalanine in the motif (1^{st}), as well as the fourth (4^{th}) and fifth (5^{th}) residue following the final proline of the motif (Ball, et al. 2002). The strongest interactions with the EVH1 domain are seen with the ActA protein, which has either an

acidic glutamic or aspartic acid in 1st position, and an acidic glutamic acid and hydrophobic leucine in the 4th and 5th position, respectively (Figure 1.5). Comparing these flanking residues to those in metavinculin, site 1 also has an aspartic acid in the 1st position, a glutamic acid in the 4th position, but has an uncharged glutamine in 5th position (Figure 1.5). Site 2, however, has a neutral glycine in 1st position, but has two aspartic acids in 4th and 5th position (Figure 1.5). It appears that the acidic residue in 1st position is a major difference between the two sites, while the acidic residues in 5th position may play a smaller role in conferring affinity.

As all of the previous binding studies which have calculated affinities for the VASP/vinculin interaction have been done solely using peptides, there is also the possibility that outside of the 14 residues examined there are other residues/sites that may be involved in mediating this interaction. Also, there could be more residues from the EVH1 domain involved in mediating the interaction than those already identified. The structure of the EVH1 domain from Mena has been solved with the 5 residue ActA peptide and in this structure, it appears that in the region where the 4th and 5th flanking residues following the final proline might lie there are two exposed arginines (Prehoda, Lee and Lim 1999). One or both of these residues may be involved in interacting with the acidic residues in the 4th and 5th position, which could provide a higher affinity, as well as confer some of the specificity that is seen between the EVH1 domain and its ligands.

Also supporting the idea that site 2 is in fact an EVH1 binding site are the results seen when the site 2 mutant is labelled with the aromatic fluorophore CPM. Amazingly, binding is increased well above that of the unlabelled mutants, to intensity levels seen with the wild-type construct (Figure 3.15B). This implies that either CPM replaces the phenylalanine or that a non-specific interaction occurs with the fluorophore. A possible

way of testing this would be to label a protein that we know does not interact with EVH1 and test it's binding, or by labelling metavinculin at a different position that is not an EVH1 binding site.

The effect of EDTA on the binding interaction was surprising: a decrease occurred with all of the constructs (Figure 3.20C). This decrease was restored when calcium was included along with the EDTA (Figure 3.20D). There are at least two possible explanations for this decrease. The first is that there is metal ion of some kind mediating or enhancing the interaction. This could help to explain why no interaction was detected with either of the fluorescence assays, as the buffer used contained EDTA. Previous experiments by other researchers were done in the absence of EDTA (Brindle, et al. 1996; Reinhard, et al. 1996). However, another possibility is that the alkaline phosphatase was damaged by EDTA, as it requires divalent cations for activity (Hermanson 1996). The development buffer of alkaline phosphatase does contain magnesium, however, which should restore the activity of the enzyme, implying that the development should be only minimally affected by the use of buffers with EDTA during binding.

4.3. Biological significance

The possibility that the second site in metavinculin contributes to VASP binding could be important in explaining the necessity for both metavinculin and vinculin expression in smooth and cardiac muscle cells. The heart is presumably the tissue which is most reliant on the expression of both of the vinculin isoforms, as it malfunctions in disorders correlated with mutations in these proteins (Maeda, et al. 1997; Olson, et al. 2002). As lack of VASP induces cardiomyopathy, it appears possible that the interaction occurring at the intercalated discs with metavinculin through both of the sites adds to the

functionality of one or both of the proteins, possibly allowing or enhancing an interaction with another ligand.

4.4. Future Directions

Future directions should include trying to obtain the full-length VASP construct to test in the solution assay, in an attempt to see if binding is increased when using a tetramer as opposed to the dimer. The fluorescence perturbation assay could also be tested using an oligomerized metavinculin construct to determine if the interaction would be detectable. Also, a full-length construct of metavinculin might reveal more about the interaction, such as whether the molecules can interact if metavinculin is in its closed conformation, or if it must be first activated. Ultimately, the mutants in a full-length metavinculin construct could be used for *in vivo* assays, detecting localization, as well as for any functional differences compared to the wild-type.

REFERENCES

Aszodi, A., Pfeifer, A., Ahmad, M., Glauner, M., Zhou, X. H., Ny, L., Andersson, K. E., Kehrel, B., Offermanns, S. and Fassler, R. (1999) The vasodilator-stimulated phosphoprotein (VASP) is involved in cGMP- and cAMP-mediated inhibition of agonist-induced platelet aggregation, but is dispensable for smooth muscle function. *EMBO J.* **18**, 37-48.

Ausubel, F. M., Brent, R., Kingston, R. E., Moore, D. D., Seidman, J. G., Smith, J. A. and Struhl, K. A. (1990) *Current Protocols in Molecular Biology*, Wiley-Interscience, Boston.

Bachmann, C., Fischer, L., Walter, U. and Reinhard, M. (1999) The EVH2 domain of the vasodilator-stimulated phosphoprotein mediates tetramerization, F-actin binding, and actin bundle formation. *J. Biol. Chem.* **274**, 23549-23557.

Bakolitsa, C., Cohen, D. M., Bankston, L. A., Bobkov, A. A., Cadwell, G. W., Jennings, L., Critchley, D. R., Craig, S. W. and Liddington, R. C. (2004) Structural basis for vinculin activation at sites of cell adhesion. *Nature* **430**, 583-586.

Ball, L. J., Jarchau, T., Oschkinat, H. and Walter, U. (2002) EVH1 domains: structure, function and interactions. *FEBS Lett.* **513**, 45-52.

Ball, L. J., Kuhne, R., Hoffmann, B., Hafner, A., Schmieder, P., Volkmer-Engert, R., Hof, M., Wahl, M., Schneider-Mergener, J., Walter, U., Oschkinat, H. and Jarchau, T. (2000) Dual epitope recognition by the VASP EVH1 domain modulates polyproline ligand specificity and binding affinity. *EMBO J.* **19**, 4903-4914.

Barstead, R. J. and Waterston, R. H. (1991) Vinculin is essential for muscle function in the nematode. *J. Cell Biol.* **114**, 715-724.

Barzik, M., Kotova, T. I., Higgs, H. N., Hazelwood, L., Hanein, D., Gertler, F. B. and Schafer, D. A. (2005) Ena/VASP proteins enhance actin polymerization in the presence of barbed end capping proteins. *J. Biol. Chem.* **280**, 28653-28662.

Bear, J. E., Loureiro, J. J., Libova, I., Fassler, R., Wehland, J. and Gertler, F. B. (2000) Negative regulation of fibroblast motility by Ena/VASP proteins. *Cell* **101**, 717-728.

Bear, J. E., Svitkina, T. M., Krause, M., Schafer, D. A., Loureiro, J. J., Strasser, G. A., Maly, I. V., Chaga, O. Y., Cooper, J. A., Borisy, G. G. and Gertler, F. B. (2002) Antagonism between Ena/VASP proteins and actin filament capping regulates fibroblast motility. *Cell* **109**, 509-521.

Belkin, A. M., Ornatsky, O. I., Glukhova, M. A. and Koteliansky, V. E. (1988) Immunolocalization of meta-vinculin in human smooth and cardiac muscles. *J. Cell Biol.* **107**, 545-553.

Birk, H. W. and Koepsell, H. (1987) Reaction of monoclonal antibodies with plasma membrane proteins after binding on nitrocellulose: renaturation of antigenic sites and reduction of nonspecific antibody binding. *Anal. Biochem.* **164**, 12-22.

Bois, P. R., O'Hara, B. P., Nietlispach, D., Kirkpatrick, J. and Izard, T. (2006) The vinculin binding sites of talin and alpha-actinin are sufficient to activate vinculin. *J. Biol. Chem.* **281**, 7228-7236.

Borgon, R. A., Vonrhein, C., Bricogne, G., Bois, P. R. and Izard, T. (2004) Crystal structure of human vinculin. *Structure* **12**, 1189-1197.

Boukhelifa, M., Parast, M. M., Bear, J. E., Gertler, F. B. and Otey, C. A. (2004) Palladin is a novel binding partner for Ena/VASP family members. Cell Motil. *Cytoskeleton* **58**, 17-29.

Brindle, N. P., Holt, M. R., Davies, J. E., Price, C. J. and Critchley, D. R. (1996) The focal-adhesion vasodilator-stimulated phosphoprotein (VASP) binds to the proline-rich domain in vinculin. *Biochem. J.* **318 (Pt 3)**, 753-757.

Butt, E., Abel, K., Krieger, M., Palm, D., Hoppe, V., Hoppe, J. and Walter, U. (1994) cAMP- and cGMP-dependent protein kinase phosphorylation sites of the focal adhesion vasodilator-stimulated phosphoprotein (VASP) in vitro and in intact human platelets. *J. Biol. Chem.* **269**, 14509-14517.

Carl, U. D., Pollmann, M., Orr, E., Gertlere, F. B., Chakraborty, T. and Wehland, J. (1999) Aromatic and basic residues within the EVH1 domain of VASP specify its interaction with proline-rich ligands. *Curr. Biol.* **9**, 715-718.

Chakraborty, T., Ebel, F., Domann, E., Niebuhr, K., Gerstel, B., Pistor, S., Temm-Grove, C. J., Jockusch, B. M., Reinhard, M. and Walter, U. (1995) A focal adhesion factor directly linking intracellularly motile Listeria monocytogenes and Listeria ivanovii to the actin-based cytoskeleton of mammalian cells. *EMBO J.* **14**, 1314-1321.

Chandrasekar, I., Stradal, T. E., Holt, M. R., Entschladen, F., Jockusch, B. M. and Ziegler, W. H. (2005) Vinculin acts as a sensor in lipid regulation of adhesion-site turnover. *J. Cell. Sci.* **118**, 1461-1472.

Chang, A. N. and Potter, J. D. (2005) Sarcomeric protein mutations in dilated cardiomyopathy. *Heart Fail. Rev.* **10**, 225-235.
Cohen, D. M., Chen, H., Johnson, R. P., Choudhury, B. and Craig, S. W. (2005) Two distinct head-tail interfaces cooperate to suppress activation of Vinculin by Talin. *J. Biol. Chem.* **280,** 17109-17117.

Cohen, D. M., Kutscher, B., Chen, H., Murphy, D. B. and Craig, S. W. (2006) A conformational switch in vinculin drives formation and dynamics of a talin-vinculin complex at focal adhesions. *J. Biol. Chem.* **281**, 16006-16015.

Coll, J. L., Ben-Ze'ev, A., Ezzell, R. M., Rodriguez Fernandez, J. L., Baribault, H., Oshima, R. G. and Adamson, E. D. (1995) Targeted disruption of vinculin genes in F9 and embryonic stem cells changes cell morphology, adhesion, and locomotion. *Proc. Natl. Acad. Sci. U. S. A.* **92**, 9161-9165.

Colosimo, A., Xu, Z., Novelli, G., Dallapiccola, B. and Gruenert, D. C. (1999) Simple version of "megaprimer" PCR for site-directed mutagenesis. *BioTechniques* **26**, 870-873.

DeMali, K. A., Barlow, C. A. and Burridge, K. (2002) Recruitment of the Arp2/3 complex to vinculin: coupling membrane protrusion to matrix adhesion. *J. Cell Biol.* **159**, 881-891.

Domann, E., Wehland, J., Rohde, M., Pistor, S., Hartl, M., Goebel, W., Leimeister-Wachter, M., Wuenscher, M. and Chakraborty, T. (1992) A novel bacterial virulence gene in Listeria monocytogenes required for host cell microfilament interaction with homology to the proline-rich region of vinculin. *EMBO J.* **11**, 1981-1990.

Eigenthaler, M., Engelhardt, S., Schinke, B., Kobsar, A., Schmitteckert, E., Gambaryan, S., Engelhardt, C. M., Krenn, V., Eliava, M., Jarchau, T., Lohse, M. J., Walter, U. and Hein, L. (2003) Disruption of cardiac Ena-VASP protein localization in intercalated disks causes dilated cardiomyopathy. *Am. J. Physiol. Heart Circ. Physiol.* **285**, H2471-81.

Fatkin, D. and Graham, R. M. (2002) Molecular mechanisms of inherited cardiomyopathies. *Physiol. Rev.* **82**, 945-980.

Geiger, B. (1979) A 130K protein from chicken gizzard: its localization at the termini of microfilament bundles in cultured chicken cells. *Cell* **18**, 193-205.

Geiger, B., Tokuyasu, K. T., Dutton, A. H. and Singer, S. J. (1980) Vinculin, an intracellular protein localized at specialized sites where microfilament bundles terminate at cell membranes. *Proc. Natl. Acad. Sci. U. S. A.* **77**, 4127-4131.

Gertler, F. B., Niebuhr, K., Reinhard, M., Wehland, J. and Soriano, P. (1996) Mena, a relative of VASP and Drosophila Enabled, is implicated in the control of microfilament dynamics. *Cell* **87**, 227-239.

Gill, S. C. and von Hippel, P. H. (1989) Calculation of protein extinction coefficients from amino acid sequence data. *Anal. Biochem.* **182**, 319-326.

Guan, K. L. and Dixon, J. E. (1991) Eukaryotic proteins expressed in Escherichia coli: an improved thrombin cleavage and purification procedure of fusion proteins with glutathione S-transferase. *Anal. Biochem.* **192**, 262-267.

Halbrugge, M. and Walter, U. (1989) Purification of a vasodilator-regulated phosphoprotein from human platelets. *Eur. J. Biochem.* **185**, 41-50.

Harbeck, B., Huttelmaier, S., Schluter, K., Jockusch, B. M. and Illenberger, S. (2000) Phosphorylation of the vasodilator-stimulated phosphoprotein regulates its interaction with actin. *J. Biol. Chem.* **275**, 30817-30825.

Hauser, W., Knobeloch, K. P., Eigenthaler, M., Gambaryan, S., Krenn, V., Geiger, J., Glazova, M., Rohde, E., Horak, I., Walter, U. and Zimmer, M. (1999) Megakaryocyte hyperplasia and enhanced agonist-induced platelet activation in vasodilator-stimulated phosphoprotein knockout mice. *Proc. Natl. Acad. Sci. U. S. A.* **96**, 8120-8125.

Hemmings, L., Rees, D. J., Ohanian, V., Bolton, S. J., Gilmore, A. P., Patel, B., Priddle, H., Trevithick, J. E., Hynes, R. O. and Critchley, D. R. (1996) Talin contains three actin-binding sites each of which is adjacent to a vinculin-binding site. *J. Cell. Sci.* **109 (Pt 11)**, 2715-2726.

Hermanson, G. T. (1996) *Bioconjugate Techniques*, Academic Press, Inc, San Diego, California.

Horton, H. R., Moran, L. A., Ochs, R. S., Rawn, J. D. and Scrimgeour, K. G. (2002) *Principles of Biochemistry,* Third ed., Prentice Hall, Upper Saddle River, NJ.

Howe, A. K., Hogan, B. P. and Juliano, R. L. (2002) Regulation of vasodilator-stimulated phosphoprotein phosphorylation and interaction with Abl by protein kinase A and cell adhesion. *J. Biol. Chem.* **277**, 38121-38126.

Huttelmaier, S., Bubeck, P., Rudiger, M. and Jockusch, B. M. (1997) Characterization of two F-actin-binding and oligomerization sites in the cell-contact protein vinculin. *Eur. J. Biochem.* **247**, 1136-1142.

Huttelmaier, S., Illenberger, S., Grosheva, I., Rudiger, M., Singer, R. H. and Jockusch, B. M. (2001) Raver1, a dual compartment protein, is a ligand for PTB/hnRNPI and microfilament attachment proteins. *J. Cell Biol.* **155**, 775-786.

Huttelmaier, S., Mayboroda, O., Harbeck, B., Jarchau, T., Jockusch, B. M. and Rudiger, M. (1998) The interaction of the cell-contact proteins VASP and vinculin is regulated by phosphatidylinositol-4,5-bisphosphate. *Curr. Biol.* **8**, 479-488.

Hyde, J. E. and Walker, I. O. (1974) The reactivity of the thiol groups of calf thymus deoxyribonucleohistone. *Nucleic Acids Res.* **1**, 203-215.

Izard, T., Evans, G., Borgon, R. A., Rush, C. L., Bricogne, G. and Bois, P. R. (2004) Vinculin activation by talin through helical bundle conversion. *Nature* **427**, 171-175.

Janssen, M. E., Kim, E., Liu, H., Fujimoto, L. M., Bobkov, A., Volkmann, N. and Hanein, D. (2006) Three-dimensional structure of vinculin bound to actin filaments. *Mol. Cell* **21**, 271-281.

Jenzora, A., Behrendt, B., Small, J. V., Wehland, J. and Stradal, T. E. (2005) PREL1 provides a link from Ras signalling to the actin cytoskeleton via Ena/VASP proteins. *FEBS Lett.* **579**, 455-463.

Johnson, R. P. and Craig, S. W. (1995) F-actin binding site masked by the intramolecular association of vinculin head and tail domains. *Nature* **373**, 261-264.

Johnson, R. P. and Craig, S. W. (1994) An intramolecular association between the head and tail domains of vinculin modulates talin binding. *J. Biol. Chem.* **269**, 12611-12619.

Johnson, R. P., Niggli, V., Durrer, P. and Craig, S. W. (1998) A conserved motif in the tail domain of vinculin mediates association with and insertion into acidic phospholipid bilayers. *Biochemistry* **37**, 10211-10222.

Kelly, D. F., Taylor, D. W., Bakolitsa, C., Bobkov, A. A., Bankston, L., Liddington, R. C. and Taylor, K. A. (2006) Structure of the alpha-actinin-vinculin head domain complex determined by cryo-electron microscopy. *J. Mol. Biol.* **357**, 562-573.

Kioka, N., Sakata, S., Kawauchi, T., Amachi, T., Akiyama, S. K., Okazaki, K., Yaen, C., Yamada, K. M. and Aota, S. (1999) Vinexin: a novel vinculin-binding protein with multiple SH3 domains enhances actin cytoskeletal organization. *J. Cell Biol.* **144**, 59-69.

Klinz, F. J. (1994) GTP-blot analysis of small GTP-binding proteins. The C-terminus is involved in renaturation of blotted proteins. *Eur. J. Biochem.* **225**, 99-105.

Krause, M., Dent, E. W., Bear, J. E., Loureiro, J. J. and Gertler, F. B. (2003) Ena/VASP proteins: regulators of the actin cytoskeleton and cell migration. *Annu. Rev. Cell Dev. Biol.* **19**, 541-564.

Krause, M., Leslie, J. D., Stewart, M., Lafuente, E. M., Valderrama, F., Jagannathan, R., Strasser, G. A., Rubinson, D. A., Liu, H., Way, M., Yaffe, M. B., Boussiotis, V. A. and Gertler, F. B. (2004) Lamellipodin, an Ena/VASP ligand, is implicated in the regulation of lamellipodial dynamics. *Dev. Cell.* **7**, 571-583.

Krause, M., Sechi, A. S., Konradt, M., Monner, D., Gertler, F. B. and Wehland, J. (2000) Fyn-binding protein (Fyb)/SLP-76-associated protein (SLAP), Ena/vasodilator-stimulated phosphoprotein (VASP) proteins and the Arp2/3 complex link T cell receptor (TCR) signaling to the actin cytoskeleton. *J. Cell Biol.* **149**, 181-194.

Kuhnel, K., Jarchau, T., Wolf, E., Schlichting, I., Walter, U., Wittinghofer, A. and Strelkov, S. V. (2004) The VASP tetramerization domain is a right-handed coiled coil based on a 15-residue repeat. *Proc. Natl. Acad. Sci. U. S. A.* **101**, 17027-17032.

Laemmli, U. K. (1970) Cleavage of structural proteins during the assembly of the head of bacteriophage T4. *Nature* **227**, 680-685.

Lanier, L. M., Gates, M. A., Witke, W., Menzies, A. S., Wehman, A. M., Macklis, J. D., Kwiatkowski, D., Soriano, P. and Gertler, F. B. (1999) Mena is required for neurulation and commissure formation. *Neuron* **22**, 313-325.

Loureiro, J. J., Rubinson, D. A., Bear, J. E., Baltus, G. A., Kwiatkowski, A. V. and Gertler, F. B. (2002) Critical roles of phosphorylation and actin binding motifs, but not the central proline-rich region, for Ena/vasodilator-stimulated phosphoprotein (VASP) function during cell migration. *Mol. Biol. Cell* **13**, 2533-2546.

Lowry, O. H., Rosebrough, N. J., Farr, A. L. and Randall, R. J. (1951) Protein measurement with the Folin phenol reagent. *J. Biol. Chem.* **193**, 265-275.

Machner, M. P., Urbanke, C., Barzik, M., Otten, S., Sechi, A. S., Wehland, J. and Heinz, D. W. (2001) ActA from Listeria monocytogenes can interact with up to four Ena/VASP homology 1 domains simultaneously. *J. Biol. Chem.* **276**, 40096-40103.

Maeda, M., Holder, E., Lowes, B., Valent, S. and Bies, R. D. (1997) Dilated cardiomyopathy associated with deficiency of the cytoskeletal protein metavinculin. *Circulation* **95**, 17-20.

Mandai, K., Nakanishi, H., Satoh, A., Takahashi, K., Satoh, K., Nishioka, H., Mizoguchi, A. and Takai, Y. (1999) Ponsin/SH3P12: an l-afadin- and vinculin-binding protein localized at cell-cell and cell-matrix adherens junctions. *J. Cell Biol.* **144**, 1001-1017.

Maru, Y., Afar, D. E., Witte, O. N. and Shibuya, M. (1996) The dimerization property of glutathione S-transferase partially reactivates Bcr-Abl lacking the oligomerization domain. *J. Biol. Chem.* **271**, 15353-15357.

Menzies, A. S., Aszodi, A., Williams, S. E., Pfeifer, A., Wehman, A. M., Goh, K. L., Mason, C. A., Fassler, R. and Gertler, F. B. (2004) Mena and vasodilator-stimulated phosphoprotein are required for multiple actin-dependent processes that shape the vertebrate nervous system. *J. Neurosci.* **24**, 8029-8038.

Niebuhr, K., Ebel, F., Frank, R., Reinhard, M., Domann, E., Carl, U. D., Walter, U., Gertler, F. B., Wehland, J. and Chakraborty, T. (1997) A novel proline-rich motif present in ActA of Listeria monocytogenes and cytoskeletal proteins is the ligand for the EVH1 domain, a protein module present in the Ena/VASP family. *EMBO J.* **16**, 5433-5444.

Olson, T. M., Illenberger, S., Kishimoto, N. Y., Huttelmaier, S., Keating, M. T. and Jockusch, B. M. (2002) Metavinculin mutations alter actin interaction in dilated cardiomyopathy. *Circulation* **105**, 431-437.

Peterson, G. L. (1977) A simplification of the protein assay method of Lowry et al. which is more generally applicable. *Anal. Biochem.* **83**, 346-356.

Petit, M. M., Fradelizi, J., Golsteyn, R. M., Ayoubi, T. A., Menichi, B., Louvard, D., Van de

Prehoda, K. E., Lee, D. J. and Lim, W. A. (1999) Structure of the enabled/VASP homology 1 domain-peptide complex: a key component in the spatial control of actin assembly. *Cell* **97**, 471-480.

Ramachandran, S. and Udgaonkar, J. B. (1996) Stabilization of barstar by chemical modification of the buried cysteines. *Biochemistry* **35**, 8776-8785.

Reinhard, M., Giehl, K., Abel, K., Haffner, C., Jarchau, T., Hoppe, V., Jockusch, B. M. and Walter, U. (1995) The proline-rich focal adhesion and microfilament protein VASP is a ligand for profilins. *EMBO J.* **14,** 1583-1589.

Reinhard, M., Rudiger, M., Jockusch, B. M. and Walter, U. (1996) VASP interaction with vinculin: a recurring theme of interactions with proline-rich motifs. *FEBS Lett.* **399**, 103-107.

Richardson, P., McKenna, W., Bristow, M., Maisch, B., Mautner, B., O'Connell, J., Olsen, E., Thiene, G., Goodwin, J., Gyarfas, I., Martin, I. and Nordet, P. (1996) Report of the 1995 World Health Organization/International Society and Federation of Cardiology Task Force on the Definition and Classification of cardiomyopathies. *Circulation* **93**, 841-842.

Rodriguez Fernandez, J. L., Geiger, B., Salomon, D. and Ben-Ze'ev, A. (1992) Overexpression of vinculin suppresses cell motility in BALB/c 3T3 cells. *Cell Motil. Cytoskeleton* **22**, 127-134.

Rual, J. F., Venkatesan, K., Hao, T., Hirozane-Kishikawa, T., Dricot, A., Li, N., Berriz, G. F., Gibbons, F. D., Dreze, M., Ayivi-Guedehoussou, N., Klitgord, N., Simon, C., Boxem, M., Milstein, S., Rosenberg, J., Goldberg, D. S., Zhang, L. V., Wong, S. L., Franklin, G., Li, S., Albala, J. S., Lim, J., Fraughton, C., Llamosas, E., Cevik, S., Bex, C., Lamesch, P., Sikorski, R. S., Vandenhaute, J., Zoghbi, H. Y., Smolyar, A., Bosak, S., Sequerra, R., Doucette-Stamm, L., Cusick, M. E., Hill, D. E., Roth, F. P. and Vidal, M. (2005) Towards a proteome-scale map of the human protein-protein interaction network. *Nature* **437**, 1173-1178.

Ruhnau, K. and Wegner, A. (1988) Evidence for direct binding of vinculin to actin filaments. *FEBS Lett.* **228**, 105-108.

Salehzada, T., Silhol, M., Lebleu, B. and Bisbal, C. (1991) Regeneration of enzyme activity after western blot: activation of RNase L by 2-5A on filter--importance for its detection. *Anal. Biochem.* **196**, 410-414.

Sambrook, J., Fritsch, E. F. and Maniatis, T. (1989) *Molecular cloning: A laboratory manual,* Cold Spring Harbour Laboratory Press, New York.

Saunders, R. M., Holt, M. R., Jennings, L., Sutton, D. H., Barsukov, I. L., Bobkov, A., Liddington, R. C., Adamson, E. A., Dunn, G. A. and Critchley, D. R. (2006) Role of vinculin in regulating focal adhesion turnover. *Eur. J. Cell Biol.* **85**, 487-500.

Sheehan, D. (1996) Fast protein liquid chromatography (FPLC) methods. *Methods Mol. Biol.* **59**, 269-275.

Skoble, J., Auerbuch, V., Goley, E. D., Welch, M. D. and Portnoy, D. A. (2001) Pivotal role of VASP in Arp2/3 complex-mediated actin nucleation, actin branch-formation, and Listeria monocytogenes motility. *J. Cell Biol.* **155**, 89-100.

Strasser, P., Gimona, M., Herzog, M., Geiger, B. and Small, J. V. (1993) Variable and constant regions in the C-terminus of vinculin and metavinculin. Cloning and expression of fragments in E. coli. *FEBS Lett.* **317**, 189-194.

Strom, A., Diecke, S., Hunsmann, G. and Stuke, A. W. (2006) Identification of prion protein binding proteins by combined use of far-Western immunoblotting, two dimensional gel electrophoresis and mass spectrometry. *Proteomics* **6**, 26-34.

Towbin, J. A. and Bowles, N. E. (2006) Dilated cardiomyopathy: a tale of cytoskeletal proteins and beyond. *J. Cardiovasc. Electrophysiol.* **17**, 919-926.

Vasile, V. C., Will, M. L., Ommen, S. R., Edwards, W. D., Olson, T. M. and Ackerman, M. J. (2006) Identification of a metavinculin missense mutation, R975W, associated with both hypertrophic and dilated cardiomyopathy. *Mol. Genet. Metab.* **87**, 169-174.

Volberg, T., Geiger, B., Kam, Z., Pankov, R., Simcha, I., Sabanay, H., Coll, J. L., Adamson, E. and Ben-Ze'ev, A. (1995) Focal adhesion formation by F9 embryonal carcinoma cells after vinculin gene disruption. *J. Cell. Sci.* **108 (Pt 6)**, 2253-2260.

Volkman, B. F., Prehoda, K. E., Scott, J. A., Peterson, F. C. and Lim, W. A. (2002) Structure of the N-WASP EVH1 domain-WIP complex: insight into the molecular basis of Wiskott-Aldrich Syndrome. *Cell* **111**, 565-576.

Walders-Harbeck, B., Khaitlina, S. Y., Hinssen, H., Jockusch, B. M. and Illenberger, S. (2002) The vasodilator-stimulated phosphoprotein promotes actin polymerisation through direct binding to monomeric actin. *FEBS Lett.* **529**, 275-280.

Weekes, J., Barry, S. T. and Critchley, D. R. (1996) Acidic phospholipids inhibit the intramolecular association between the N- and C-terminal regions of vinculin, exposing actin-binding and protein kinase C phosphorylation sites. *Biochem. J.* **314 (Pt 3)**, 827-832.

Weller, P. A., Ogryzko, E. P., Corben, E. B., Zhidkova, N. I., Patel, B., Price, G. J., Spurr, N. K., Koteliansky, V. E. and Critchley, D. R. (1990) Complete sequence of human vinculin and assignment of the gene to chromosome 10. *Proc. Natl. Acad. Sci. U. S. A.* **87**, 5667-5671.

Wilce, M. C. and Parker, M. W. (1994) Structure and function of glutathione S-transferases. *Biochim. Biophys. Acta* **1205**, 1-18.

Witt, S., Zieseniss, A., Fock, U., Jockusch, B. M. and Illenberger, S. (2004) Comparative biochemical analysis suggests that vinculin and metavinculin cooperate in muscular adhesion sites. *J. Biol. Chem.* **279**, 31533-31543.

Wood, C. K., Turner, C. E., Jackson, P. and Critchley, D. R. (1994) Characterisation of the paxillin-binding site and the C-terminal focal adhesion targeting sequence in vinculin. *J. Cell. Sci.* **107 (Pt 2)**, 709-717.

Xu, W., Baribault, H. and Adamson, E. D. (1998) Vinculin knockout results in heart and brain defects during embryonic development. *Development* **125**, 327-337.

Yamada, S., Pokutta, S., Drees, F., Weis, W. I. and Nelson, W. J. (2005) Deconstructing the cadherin-catenin-actin complex. *Cell* **123**, 889-901.

Yan, H., Lim, J. T., Contillo, L. G. and Krolewski, J. J. (1995) Glutathione S-transferase fusion proteins mimic receptor dimerization in permeabilized cells. *Anal. Biochem.* **231**, 455-458.

Zamir, E. and Geiger, B. (2001) Molecular complexity and dynamics of cell-matrix adhesions. *J. Cell. Sci.* **114**, 3583-3590.

Zhang, Y., Tu, Y., Gkretsi, V. and Wu, C. (2006) Migfilin interacts with vasodilator-stimulated phosphoprotein (VASP) and regulates VASP localization to cell-matrix adhesions and migration. *J. Biol. Chem.* **281**, 12397-12407.

Zimmermann, J., Kuhne, R., Volkmer-Engert, R., Jarchau, T., Walter, U., Oschkinat, H. and Ball, L. J. (2003) Design of N-substituted peptomer ligands for EVH1 domains. *J. Biol. Chem.* **278**, 36810-36818.

Zimmermann, J., Labudde, D., Jarchau, T., Walter, U., Oschkinat, H. and Ball, L. J. (2002) Relaxation, equilibrium oligomerization, and molecular symmetry of the VASP (336-380) EVH2 tetramer. *Biochemistry* **41**, 11143-11151.